

# Symmetry group factorization reveals the structure-function relation in the neural connectome of *Caenorhabditis elegans*

Flaviano Morone<sup>1</sup> and Hernán A. Makse<sup>1</sup>

<sup>1</sup>*Levich Institute and Physics Department,  
City College of New York, New York, NY 10031*

## Abstract

The neural connectome of the nematode *Caenorhabditis elegans* has been completely mapped, yet in spite of being one of the smallest connectomes (302 neurons), the design principles that explain how the connectome structure determines its function remain unknown. Here, we find symmetries in the locomotion neural circuit of *C. elegans*, each characterized by its own symmetry group which can be factorized into the direct product of normal subgroups. The action of these normal subgroups partitions the connectome into sectors of neurons that match broad functional categories. Furthermore, symmetry principles predict the existence of novel finer structures inside these normal subgroups forming feedforward and recurrent networks made of blocks of imprimitivity. These blocks constitute structures made of circulant matrices nested in a hierarchy of block-circulant matrices, whose functionality is understood in terms of neural processing filters responsible for fast processing of information.

## I. INTRODUCTION

There is growing consensus in present day complexity science that functions of living networked systems are controlled by the structure of interconnections between the network components [1–3]. Under this assumption, the problem of understanding how function emerges from structure [4] can be cast in terms of the network structure itself, and this problem is, fundamentally, of a theoretical nature. Here we address this problem by considering the connectome of the neural system of the nematode *C. elegans*, a prototypical model connectome displaying complex behavior [5–11].

Specifically, we show that the building blocks of the locomotion part of the connectome are mathematically defined via its ‘*symmetry group*’ [12]. The implications of this result are two-fold. First, we show that the symmetry group of locomotion circuits can be broken down into a unique factorization as the *direct product* of smaller ‘*normal subgroups*’ [12, §1.6]. These normal subgroups directly determine the separation of neurons into sectors. The biological significance of this result is measured by the fact that these sectors of neurons match known functional categories of the connectome. Second, we show that the sectors of neurons defined by the normal subgroups of the connectome can be further decomposed into ‘*blocks of imprimitivity*’ [12, §1.5] made of ‘*circulant*’ matrices [13, §3]. These circulant matrices are processing units encoding for fast signal filtering and oscillations in the locomotion function. Figure 1a-g defines the group theoretical concepts of permutation symmetry, normal subgroup, block of imprimitivity and circulant matrix needed to understand the theoretical basis of the structure-function relation in the connectome that we present here.

Our fundamental result is that symmetries of neural networks have a direct biological meaning, which can be rigorously justified using the mathematical formalism of symmetry groups. This formalism makes possible to understand the significance of the structure-function relationship: the rationale behind the locomotion function in *C. elegans* is the existence of symmetries in the connectome which uniquely assign neurons to functional categories defined through the mechanism of factorization of the symmetry group. Therefore, the structure-function relationship theoretically follows from a symmetry principle. Although the specific form of the symmetry group is different in different functions, the basic ideas and methods of our formalism are the same and can be tested for any system. The symmetry group of a network has also a strong impact on the dynamics of the sys-

tem. That is, it determines the synchronization of neurons belonging to the same orbit defined by the symmetry group [14, 15]. Furthermore, the form of synchrony determined by the symmetries of the connectivity structure is largely independent of the specific details of the neural dynamics. Seen globally, network symmetries may help to reveal the general principles underlying the mechanism of neural coding engraved in the connectome.

## II. RESULTS

### A. Neural connectome: symmetry groups

The neuronal network of the hermaphrodite *C. elegans* contains 302 neurons, which are individually identifiable, and the wiring diagram includes 890 gap junctions and 6393 chemical synapses [9]. The number of neurons across animals is very consistent [5, 9], while the gap-junctions and chemical synapses are reproducible within 25% variability from animal to animal [5, 9, 16, 17]. Due to its small size and relative completeness, the neural network of *C. elegans* has been a formidable model system to search for design principles underpinning the structural organization and functionality of neural networks [5–11].

We examine the forward and backward locomotion functions in *C. elegans* which have been well-characterized in the literature [5–7, 10, 11, 18–20]. The locomotion is supported by two main functional classes of neurons called (1) command interneurons and (2) motor neurons (in addition to sensory neurons which are not studied here). The backward locomotion of the animal is supported by the activation of interneurons AVA, AVE, and AVD [18] and AIB and RIM [10], and motor neuron classes VA and DA. Similarly, forward locomotion is supported by the activation of motor neuron classes VB and DB through the interneuron classes AVB and PVC [5, 6, 10, 18, 19] and RIB [10]. We use the most up-to-date connectome of gap-junctions and chemical synapses from Ref. [9] to construct the neural circuits of forward and backward locomotion (details in Supplementary Note 1. We represent the synaptic connectivity structure by the weighted adjacency matrix  $A_{ij} \neq 0$  if neurons  $i$  connects to  $j$ , and  $A_{ij} = 0$  otherwise. Gap-junctions are undirected links,  $A_{ij} = A_{ji}$ , and chemical synapses are directed.

To explain the concept of symmetries and the procedure for finding the symmetry group, we first consider the circuit comprising only the interneurons connected via gap-junctions

involved in the forward task (Fig. 1a, adjacency matrix in Fig. 1b, weights on the links represent the number of connections provided in [9]). Later, we will see how this circuit is integrated in the full connectome.

This sub-circuit contains  $4! = 24$  possible permutations of its 4 neurons. Out of these 24, only 8 are permutation symmetries as shown in Fig. 1c. A permutation symmetry, or automorphism [12, 15, 21, 22], is a transformation defined as a permutation of neurons which preserves the connectivity structure  $A$  (see Supplementary Note 2 for detailed definition). This means that before and after the application of an automorphism, the neurons are connected exactly to the same neurons. Mathematically, if  $P$  is an automorphism, then the permuted adjacency matrix  $PAP^{-1}$  is equal to the original one,  $PAP^{-1} = A$ , or, equivalently,  $P$  and  $A$  commute with each other:

$$[P, A] \equiv PA - AP = 0 \quad \Longleftrightarrow \quad P \text{ is a symmetry} . \quad (1)$$

For instance, the permutation  $ABVL \leftrightarrow RIBR$  and  $ABVR \leftrightarrow RIBL$  represented by  $P_6$  in Fig. 1c is an automorphism since it leaves the connectivity intact. The set of automorphisms forms the symmetry group of the circuit, which, in this case, is the dihedral group  $\mathbf{D}_8$ , which is the group of symmetries of a square [12]. To be called a group of transformations, the transformations need to satisfy four axioms: (1) the existence of an inverse in the group, (2) the existence of an identity, (3) the associative law, and (4) the composition law. In addition, if the transformations are commutative, then the group is called abelian.

## B. Pseudosymmetries

The study of the full locomotion circuit requires a generalization of the notion of network symmetry, which we call ‘pseudosymmetry’. The concept of pseudosymmetry arises naturally from the observation that connectomes vary from animal to animal, so no two worms will ever have the same connectome [5, 9, 16, 17]. This variation is estimated experimentally to be 25% of the total connections from worm to worm, as reported in [9] using data from [5, 16, 17]. We consider this variability across individual connectomes as an intrinsic property consistent with biological diversity and evolution. Furthermore, the number of connections is subject to change from animal to animal through plasticity, learning and memory [23], so it cannot be ignored. On the other hand, while connectomes vary from an-



imal to animal, functions developed from them, such as forward and backward locomotion, are barely distinguishable across different worms, and still show some vestige of an ideal symmetry. In fact, the locomotion function is preserved despite the 25% variation in the connectomes. Consequently, we expect that deviations from exact symmetries to be relatively 'small'. Exact symmetries of the connectome should be considered as an idealization, and we do not expect them to be realized exactly.

Therefore, we consider pseudosymmetries of the connectome rather than perfect symmetries. Unlike perfect symmetries, defined by the abelian commutator Equation (1) and shown in the circuit of Fig. 1a, the definition of pseudosymmetry depends on an additional parameter, a small number  $\varepsilon > 0$ . This parameter quantifies the uncertainty in the connectivity structure of the connectome due to natural variations across animals, and, thus, we call it the '*uncertainty constant*' of the connectome. A pseudosymmetry is an approximate automorphism  $P_\varepsilon$ , in the sense that the commutator Equation (1) is replaced by a non-zero but small  $\varepsilon$ -norm (detailed definition in Supplementary Note 3):

$$||[P_\varepsilon, A]|| < \varepsilon M \iff P_\varepsilon \text{ is a pseudosymmetry}, \quad (2)$$

where  $M$  is the total number of network links including weights.  $P_\varepsilon$  approximates an exact symmetry in the ideal limit  $\varepsilon \rightarrow 0$ . The norm of the commutator, denoted as  $||[P_\varepsilon, A]||$ , measures the number of links where  $P_\varepsilon$  and  $A$  fail to commute given an upper limit tolerance  $\varepsilon$  in the fraction of links for the failure of commutativity (a simple pseudosymmetry is exemplified in Fig. 1d). The norm of the commutator in Equation (2) is defined as the  $L_1$  norm, denoted as  $||[P, A]||$ , and given by the following equation:

$$||[P, A]|| = ||PA - AP|| = ||A - PAP^{-1}|| = \sum_{ij} |A_{ij} - A_{P(i)P(j)}|, \quad (3)$$

where the last equality follows from the fact that  $P$  is an isometry (i.e.  $||A|| = ||PAP^{-1}||$  for any matrix  $A$ ). We see that this definition of pseudosymmetry via a commutator resembles the uncertainty principle in quantum mechanics and, thus, perfect symmetries correspond to the 'classical limit' of the pseudosymmetries.

Equation (2) means that a pseudosymmetry must preserve at least a fraction  $(1 - \varepsilon)$  of network links. The set of pseudosymmetries of the connectome contains not only the symmetry group of the connectome ( $\varepsilon = 0$ ) but it is augmented by the permutations that are 'almost' automorphisms. We note that the set of pseudosymmetries does not form a group

by itself, since the pseudosymmetries do not satisfy the composition law. For instance, two pseudosymmetries (which by definition are below the threshold  $\varepsilon$ ) may be composed into a third pseudosymmetry that breaks more than a fraction of  $\varepsilon$  contacts, and, thus, does not belong to the original set of pseudosymmetries, violating composition.

Knowledge of the pseudosymmetries is particularly useful for understanding the robustness of functions under small perturbations of the connectome. This property makes it analogous to the concept of pseudospectrum which tells how much the spectrum of eigenvalues of a matrix moves respect to small perturbations, see [24, §2.8.1]. Simply put, if the set of pseudosymmetries is clustered around the ideal symmetry group (i.e., the uncertainty constant is small), network functions are robust under small perturbations. Conversely, if it is widely spread, then functions are more likely to be lost under small perturbations. Having all concepts at hand, we move to discuss the whole forward and backward circuits and their symmetries, which, hereafter, are meant to be pseudosymmetries, although we keep using the shorthand ‘symmetry’ for lexical convenience.

The forward gap-junction circuit is shown in Fig. 2. This circuit has permutation symmetries, denoted as  $\mathbf{F}_{\text{gap}}$ , most of which can be spotted by eye in the layout displayed in the figure. Figures 2a and 2b display the real circuit, the adjacency matrix and its pseudosymmetries (details of calculations in Supplementary Note 3). The uncertainty constants  $\varepsilon$  of these pseudosymmetries are listed in Table I and fall below the upper experimental limit of 25%. Thus, all pseudosymmetries have biological significance. Figures 2c and 2d show an ideal circuit obtained by setting  $\varepsilon = 0$  compatible with the found pseudosymmetries (see Supplementary Note 3 for details on how to obtain the ideal symmetric circuit).

### C. Symmetry group factorization into normal subgroups

The crucial property of the symmetry group  $\mathbf{F}_{\text{gap}}$  is its factorization into smaller ‘*normal subgroups*’. Its importance derives from the fact that these normal subgroups match the known broad functional categories of neurons involved in locomotion, such as command interneurons, motor and touch neurons [25]. A ‘*subgroup*’  $\mathbf{H}$  of a group  $\mathbf{G}$  is a subset of transformations of  $\mathbf{G}$  which forms itself a group, i.e., the transformations satisfy the four axioms of a group.

To understand what a normal subgroup is, we consider, for instance, the automorphism

that exchanges the motor neurons  $\sigma : (\text{VB2, DB3, DB2, VB1}) \leftrightarrow (\text{DB1, VB4, VB5, VB6})$  and forms (with the identity) the dihedral group  $\mathbf{D}_1$  (Figs. 2a and 2b). Importantly, this automorphism acts independently only on neurons (VB2, DB3, DB2, VB1, DB1, VB4, VB5, VB6), and leaves the rest of the neurons of the connectome intact. Likewise, the automorphism  $\tau : \text{VB7} \leftrightarrow \text{VB3}$  forms another group by itself, called the cyclic group of order 2,  $\mathbf{C}_2$ , and also acts independently on this set of neurons and not on others.

The property of acting independently on a subset of neurons means that  $\mathbf{D}_1$  (and  $\mathbf{C}_2$ ) forms itself a smaller group, called a ‘*normal subgroup*’ inside the full symmetry group  $\mathbf{F}_{\text{gap}}$ . More formally, a subgroup  $\mathbf{H}$  is said to be normal in a group  $\mathbf{G}$  if and only if  $\mathbf{H}$  commutes with every element  $g \in \mathbf{G}$ , i.e.,  $[g, \mathbf{H}] = g\mathbf{H} - \mathbf{H}g = 0$ . The formal definition of subgroup and normal subgroup are explained in Supplementary Note 4, see [12, §1.6].

This property implies that the group  $\mathbf{F}_{\text{gap}}$  can be factorized in a unique way as a direct product of its two normal subgroups as:  $\mathbf{D}_1 \times \mathbf{C}_2$  (definition of factorization of a group in Supplementary Note 4, see [12, §1]). The significance of the normal subgroup is that the normal transformations identify a unique and non-overlapping subset of neurons that are moved by each normal subgroup. This set of neurons are called the ‘*sector*’ associated with the normal subgroup. Since each normal subgroup acts only on an independent sector, the factorization of groups into normal subgroups leads also to a partition of neurons into unique disjoint sectors.

In simple terms, this means that when an automorphism in a normal subgroup is applied to the network, only the neurons in the sector of the normal subgroup are permuted, while the rest of the neurons that are outside the sector are not affected. Thus, we say that the normal subgroup automorphisms act only on the neurons belonging to its sector providing a unique separation and classification of the neurons and the associated factorization of the symmetry group. This factorization is mathematically analogous to the unique factorization of natural numbers into primes, and this notion is extended to group theory for those finite groups that can be factorized into ‘prime’ normal subgroups, as it is the case of the connectome.

The symmetry group  $\mathbf{F}_{\text{gap}}$  is factorized as a direct product of 6 normal subgroups as:

$$\mathbf{F}_{\text{gap}} = [\mathbf{C}_2 \times \mathbf{C}_2] \times [\mathbf{S}_5 \times \mathbf{D}_1 \times \mathbf{C}_2 \times \mathbf{C}_2] . \quad (4)$$

Each subgroup acts on a non-overlapping independent sector of neurons as indicated in Fig. 2 (see also Supplementary Note 5). Table I lists the uncertainty constant for each subgroup

of pseudosymmetries indicating that all  $\varepsilon$  are small and below the experimental upper limit 25% [5, 9, 16, 17].

The factorization of the symmetry group  $\mathbf{F}_{\text{gap}}$  in Equation (4) is significant because it determines a partition of the circuit into sectors that match specific categories of neurons [25]. To define the functional categories or classes of neurons we follow the literature where functions have been determined experimentally and compiled at the WormAtlas [25]. Broad functional categories of neurons are provided at <http://www.wormatlas.org/hermaphrodite/nervous/Neuroframeset.html>, Chapter 2.2. A classification for every neuron into four broad neuron categories follows: (1) motor neurons, (2) sensory neurons, (3) interneurons, and (4) polymodal neurons. A function is assigned to each neuron based on this experimental classification into neuron categories. This classification is displayed in Supplementary Table 1 and Supplementary Table 2, and discussed in Supplementary Note 6. These categories represent the ground truth to test the predictions of our theory.

Specifically, the factor  $[\mathbf{C}_2 \times \mathbf{C}_2]$  corresponds to the command interneuron category and comprises command interneurons which drive the forward locomotion: AVBL, ABVR and RIBL, RIBR. The entire motor class is associated to an entire independent factor  $[\mathbf{S}_5 \times \mathbf{D}_1 \times \mathbf{C}_2 \times \mathbf{C}_2]$ , and includes all motor neurons innervating the muscle cells responsible for the undulatory motion of *C. elegans*.

Applying the same symmetry procedure, we find that all forward/backward gap-junction/chemical synapse circuits form symmetry groups, and these groups can be factorized into normal subgroups in the same way as in Equation (4) (see Fig. 3 and Fig. 4 and Supplementary Note 5 for details). The correspondence between neuron sectors from group theory and known categories of neurons occurs consistently across all circuits, and further includes a subgroup related to touch sensitivity [6] in the forward (PVCL, PVCR, Fig. 4a) and backward (AVDL, AVDR, Fig. 4c) chemical synaptic circuits. The full list of sectors, normal subgroups and uncertainty constants of the pseudosymmetries are provided in Table I.

The normal subgroups partition the connectome into non-overlapping functional sector of neurons, thus realizing the segregation of function. At the same time, the sectors remain connected in the connectome without breaking the symmetries, thus fulfilling the integration of function into a globally connected network. Thus, the symmetric subgroup organization of the connectome provides an elegant solution to the conundrum of functional specialization in the presence of a global integration of information necessary for efficient coherent

function [26], a profound issue in neuroscience

While group factorization can distinguish different classes of neurons, this distinction may also be seen in some cases by directly looking at the adjacency matrix: for instance in Fig. 2b the AVB interneurons are heavily connected hub neurons which could be, in principle, also distinguished by any connectivity measure. That is, the neurons AVBL and AVBR are hubs with large degree  $k = 18$  and are easily distinguished from the rest of the neurons which have generally smaller degree. However, in general, having the same degree does not imply that the neurons belong to the same subgroup. Thus, the connectivity measure alone may not fully capture the symmetry groups that we find.

For instance, neurons can be in the same sector subgroup and at the same time could, in principle, have different degree. This situation is seen for example in the neurons of the forward motor sector subgroup  $\mathbf{D}_1$  in Fig. 2a and 2c. In the circuit of Fig. 2c, the neurons in  $\mathbf{D}_1$  have different degree: VB5, DB2 VB4 and DB3 with  $k = 5$ , VB1 and VB6 with  $k = 3$ , VB2 and DB1 with  $k = 8$ . Thus, even though these neurons have different degree, they belong to the same subgroup and functional class: the motor sector subgroup  $\mathbf{D}_1$ . In general, the degree alone is not enough to separate the neurons in subgroups and known classes.

Furthermore, Fig. 2b shows that the pair (VB8, VB9) has the same connectivity as the pair (RIBL, RIBR), and thus they could be classified in the same category as either motor neuron (with VB) or interneurons (with RIB). If we consider the neurons unweighted they merge into the same subgroup and they should perform the same function. However, considering the weights, there is an asymmetry, since both, VB9 and VB8 have 6 and 7 connections to AVBL and AVBR respectively, while RIBL and RIBR have one connection each to both neurons (see Supplementary Fig. 3). Indeed, the WormAtlas classifies RIBL and RIBR as interneurons [25], thus, we classify these pairs of neurons in different classes. The asymmetry in the weights might be the reason why the experiments compiled at the WormAtlas find that these two set of neurons may work in different categories: motor and interneuron. In general, it is possible for a neuron to be involved in multiple functions. The case of polymodal neurons can be treated theoretically by generalizing the direct-product factorization to semidirect-product factorization of normal and non-normal subgroups. Semi-direct product factorization could capture overlapping sectors of neurons and multi-functionality which are more prevalent across the connectome beyond locomotion.

#### D. Statistical significance of the symmetry subgroups

To establish the degree to which the symmetries of the locomotion sub-circuits are statistically significant, we compare the symmetry subgroups against control random sub-circuits. Indeed, a high enough value of  $\epsilon$  would yield an approximate symmetric version of any arbitrary circuit: a fully random non-symmetric connectome implies  $\epsilon = 1$ , and a perfect symmetric one  $\epsilon = 0$ . In between, all networks can be classified by their  $\epsilon$ -value. Thus, it is important that not only  $\epsilon$  be smaller than the experimental variability  $\epsilon < 25\%$ , but also be statistically significant. Statistical metrics to evaluate the symmetries are p-value statistical tests to compare results with a randomized null model preserving the degree sequence. Specifically, the p-value of a pseudo-symmetry subgroup  $G_\epsilon$  is defined as the probability to find a subgroup  $G_{\epsilon^*}$  with  $\epsilon^* \leq \epsilon$  in a randomized circuit with the same degree sequence as the real circuit. The results of the p-values are summarized in Table I for each subgroup, showing that pseudosymmetry subgroups are, indeed, statistically significant.

#### E. Comparison with other methods to find functional modules

It is interesting to compare the functional partition obtained by the symmetries of the connectome with typical modularity detection algorithms which are widely used to identify functional modules in biological networks [27]. Indeed, there is a large body of work which examines the connectivity of biological networks to algorithmically classify the constituent neurons into modules and compare those modules to known classifications. Therefore, below we investigate how symmetry detected sectors compare to existing algorithms such as modularity and community detection, and other centrality measures.

We run the Louvain community detection algorithm [28] on the forward and backward circuit and find the modular partition seen in Fig. 5. We find that modules identified by the Louvain algorithm do not generally capture the functional modules identified by symmetry subgroups, nor the experimental classification into neural functions.

Typically, the modularity algorithm assigns to the same functional module a hub-like interneuron AVBR together with its connected neurons in the motor sector (see Fig. 5a), since these neurons are all highly connected. Thus, the modularity algorithm will typically mix the interneuron and motor sectors. Symmetry factorization into normal subgroups,

on the other hand, correctly classifies AVBL and AVBR separately from the VB and DB neurons in the motor sector, even though these sectors are well connected. Similar results are obtained when we use other network centralities: Fig. 5b and 5d show the modules obtained by ranking neurons according to eigenvector centrality. We find that such centrality measure does not capture the partition into symmetry sectors nor the functional classes.

#### F. A recurrent and feedforward neural network made of blocks of imprimitivity and circulant matrices

The data analyzed so far indicate that there is still a more refined structure inside the broad functional categories of motor, command and touch, that requires further exploration. For instance, the motor class of forward gap junctions (Fig. 2) consists of 4 different normal subgroups:  $[\mathbf{S}_5 \times \mathbf{D}_1 \times \mathbf{C}_2 \times \mathbf{C}_2]$ . Next, we show that the functionality of this finer structure can be systematically obtained through a more refined group theoretical concept of ‘*block of imprimitivity*’ [12, §3], which identifies the fundamental processing units of the connectome and naturally leads to a novel functionality in terms of mechanism of neural coding.

A block of imprimitivity is a set of neurons that, under the action of the automorphisms of a subgroup, is completely mapped onto itself or it is mapped onto a completely disjoint set of neurons (formal definition of block of imprimitivity in Supplementary Note 7, see [12, §1.5], and Fig. 1f). For instance, consider the subgroup  $\mathbf{D}_1$  of the forward gap-junction circuit (Fig. 2) which consists of the automorphism  $\sigma \in \mathbf{D}_1$  which acts on the sector (VB2, DB3, DB2, VB1, DB1, VB4, VB5, VB6). The subset of neurons highlighted in green in Fig. 2c,  $\mathcal{B}_1 = (\text{VB2, DB3, DB2, VB1})$ , forms a block of imprimitivity since  $\sigma$  moves this set into a different one, highlighted in black,  $\mathcal{B}_2 = (\text{DB1, VB4, VB5, VB6})$ , which is the other block of imprimitivity of the sector and a conjugate block of  $\mathcal{B}_1$ . These two blocks form the so-called *system of imprimitivity*, a fundamental concept in group theory [12, 29]. The other normal subgroups of the forward circuit do not have a nontrivial block system of imprimitivity, hence they are said to be *primitive* (Supplementary Note 7, [12, §3]).

The resulting block partition of each adjacency matrix is shown in Figs. 2d, 3d, 4b and 4d. These systems of imprimitivity identify new functionalities in each locomotion circuit. Specifically, we find that the system of imprimitivity of each locomotion circuit is formed by blocks represented by *circulant* matrices [13]. A circulant matrix is a square matrix

where each row is a cycle shift to the right of the row above it, and wrapped around [13, §3] (see Methods Section for definition). In alignment with pseudosymmetries, the circulant matrices are interpreted as pseudocirculant matrices of the real circuit. A pseudocirculant matrix differs from a circulant matrix by a fraction  $\varepsilon$  of their links. We note that this partition into blocks of imprimitivity is not unique. For instance, another possible block system corresponds to a partition made by the orbits.

Circulant matrices are well-known in the field of digital signal processing, recurrent and feedforward neural networks [4] and cryptography, and are widely used as efficient linear filters to solve a variety of tasks in digital image processing, most notably as edge-detection and signal compression [4, 30], but also in tracking [31], voice recognition, and computer vision [32]. Circulant matrices are the kernels of discrete convolutions and are used in discrete Fourier transform to solve efficiently systems of linear equations in nearly linear time [13] that significantly speed up the  $O(N^3)$  arithmetic complexity of Gaussian elimination.

We find different types of circulant matrices in the connectome which are, in turn, nested into larger block-circulant matrices (see definitions in Fig. 1b and Fig. 2d and Methods Section). Two circulant matrices occur consistently in all locomotion circuits and act as a ‘high-pass’ filter:

$$\mathcal{H} = \text{circ}(0, 1) = \begin{bmatrix} 0 & 1 \\ 1 & 0 \end{bmatrix}, \quad (5)$$

and a ‘low-pass’ filter:

$$\mathcal{L} = \text{circ}(1, 1) = \begin{bmatrix} 1 & 1 \\ 1 & 1 \end{bmatrix}. \quad (6)$$

The third type of circulant matrix represents a 4-cycle permutation:

$$\mathcal{F} = \text{circ}(0, 1, 0, 1) = \begin{bmatrix} 0 & 1 & 0 & 1 \\ 1 & 0 & 1 & 0 \\ 0 & 1 & 0 & 1 \\ 1 & 0 & 1 & 0 \end{bmatrix}, \quad (7)$$

and acts on the blocks of imprimitivity  $\mathcal{B}_1$  and  $\mathcal{B}_2$  in the motor sector of the forward gap-junction circuit (Figs. 2c and 2d). Intuitively, each circulant matrix represents a cycle embedded in the subgroup sector as seen in Fig. 2c for  $\mathcal{B}_1$ :  $\text{VB2} \rightarrow \text{DB3} \rightarrow \text{DB2} \rightarrow \text{VB1} \rightarrow \text{VB2}$ . In the same figure we see the 4-cycle of the conjugate block  $\mathcal{B}_2$ .



The  $2 \times 2$  circulant matrix  $\mathcal{H}$  in Equation (5) is quite ubiquitous and corresponds to a 2-cycle (or transposition). For instance, the 2-cycle  $\text{VB8} \rightarrow \text{VB9} \rightarrow \text{VB8}$  in the forward gap junction circuit Fig. 2c forms a circulant matrix of the form given by  $\mathcal{H}$ . This is also a block of imprimitivity, since this block is the only one inside the subgroup  $\mathbf{C}_2$ . Subgroup  $\mathbf{S}_5$  also forms a circulant matrix, although a trivial one in this case since all its elements are zero.

It is interesting to see that the circulant matrices are nested into an structure of block-circulant matrices (see Methods Section for definition), suggesting a hierarchical organization of building blocks in the connectome. Typical block-circulant matrices are of the form [13]:

$$\mathcal{BC} = \text{bcirc}(\mathcal{H}, \mathcal{L}) = \begin{bmatrix} \mathcal{H} & \mathcal{L} \\ \mathcal{L} & \mathcal{H} \end{bmatrix} = \begin{bmatrix} 0 & 1 & 1 & 1 \\ 1 & 0 & 1 & 1 \\ 1 & 1 & 0 & 1 \\ 1 & 1 & 1 & 0 \end{bmatrix}. \quad (8)$$

For instance, this block-circulant matrix appears in the command sector of the forward gap junction circuit between the neurons RIBL, RIBR, AVBL, AVBR. This is seen in Fig. 1b and also in Fig. 2d. It is interesting to note that when we analyze the group structure of the interneuron only circuit of gap junctions, then we find the group structure shown in Fig. 1b. When we integrate this circuit in the full forward circuit, then this group becomes a system of imprimitivity shown as  $\mathcal{B}_6$  and  $\mathcal{B}_7$  in Fig. 2d. This is a block-circulant matrix made itself by circulant matrices forming a nested hierarchical structure. This hierarchical nestedness is repeated across all the connectome.

A block-circulant structure is formed by the imprimitive blocks  $\mathcal{B}_1$  and  $\mathcal{B}_2$  in the same forward gap junction circuit, Fig. 2d. In this case, we have:

$$A_1 = \mathcal{F} = \text{circ}(0, 1, 0, 1) = \begin{bmatrix} 0 & 1 & 0 & 1 \\ 1 & 0 & 1 & 0 \\ 0 & 1 & 0 & 1 \\ 1 & 0 & 1 & 0 \end{bmatrix}, \quad \text{and} \quad A_2 = \begin{bmatrix} 0 & 0 & 0 & 1 \\ 0 & 0 & 0 & 0 \\ 0 & 1 & 0 & 0 \\ 0 & 0 & 0 & 0 \end{bmatrix}, \quad (9)$$

and both  $\mathcal{B}_1$  and  $\mathcal{B}_2$  combine into a block-circulant matrix of the form:

$$\mathcal{BC} = \text{bcirc}(A_1, A_2). \quad (10)$$

Also,  $\mathcal{B}_6$  and  $\mathcal{B}_7$  in the backward gap junction circuit of Fig. 3d composed of neurons AIBL, AIBR, RIML, RIMR form a block-circulant matrix

$$\mathcal{BC} = \text{bcirc}(A_1, A_2) \quad (11)$$

with

$$A_1 = \text{circ}(0, 0), \quad \text{and} \quad A_2 = \text{circ}(1, 0) = \begin{bmatrix} 1 & 0 \\ 0 & 1 \end{bmatrix}. \quad (12)$$

These results suggest that we can think of the connectome as a feedforward network made of interneurons that feeds a recurrent network in the motor system [4] made of a system of sensing operators, each represented by an imprimitive block with a circulant structure. Such a feed-forward and recurrent network architecture is universally seen across many neural systems and it is used as a model of the receptive fields in the primary visual cortex [4]. Such a system can be modeled by a feedforward matrix  $\mathbf{W}$  and a recurrent network  $\mathbf{M}$  processing the input activity  $\mathbf{u}$  to the output  $\mathbf{v}$  as a linear filter, see Dayan & Abbott [4]:

$$\tau \frac{d\mathbf{v}}{dt} = -\mathbf{v} + \mathbf{M}\mathbf{v} + \mathbf{W}\mathbf{u}, \quad (13)$$

where  $\tau$  is a time characteristic. The crucial property of this system is that the matrix  $\mathbf{M}$  contains loops in the network.

For instance, in the case of the gap junction forward circuit (Fig. 2), the AVBL and AVBR interneurons act as the input layer  $\mathbf{u} = (u_{\text{AVBL}}, u_{\text{AVBR}})^T$  which is first processed by the feedforward matrix represented by a fully connected matrix:

$$\mathbf{W} = \begin{bmatrix} 1 & 1 \\ 1 & 1 \\ 1 & 1 \\ 1 & 1 \end{bmatrix}, \quad (14)$$

whose output is then processed by the recurrent network in the motor sector by, for instance, processing the signal in the motor neurons of the imprimitivity block  $\mathcal{B}_1$ ,  $\mathbf{v} = (v_{\text{VB2}}, v_{\text{DB3}}, v_{\text{DB2}}, v_{\text{VB1}})^T$  by the recurrent circulant matrix  $\mathbf{M} = \mathcal{F} = \text{circ}(0, 1, 0, 1)$  from Equation (8). The same signal processing occurs in the feedforward and recurrent network formed by the conjugate motor imprimitive block  $\mathcal{B}_2$ . Similar structure is seen in the backward circuit Fig. 3 with AVAL-AVAR feed-forwarding information into the recurrent circulant blocks in the motor sector. The chemical circuits also contain such a feed-forward and recurrent structure: PVCL-PVCR feeds the forward motor circulant blocks (Fig. 4a) and AVE-AVD-AVA feed the backward motor circulant blocks (Fig. 4c).

Using the language of signal processing in computational neuroscience, these recurrent networks are analogous to the core of receptive fields that process information in the visual

cortex, see Dayan & Abbott [4]. For instance a widely used filter in signal processing is the edge-detector [4, 30] which employs a circulant matrix defined by  $\mathbf{M} = \text{circ}(0, 1, -1, 0, \dots, 0)$  to compute a ‘derivative’ of the spatial signal and detect sharp edges [4]. Another typical computation is performed by a circulant matrix  $\mathbf{M} = \text{circ}(0, 1, -2, 1, 0, \dots, 0)$  to represent a second derivative of the signal, and so on.

In the case of the connectome, one possible interpretation of the purpose of the found circulant filters is to separate one band of frequencies from another and perform signal compression. The high-pass filter  $\mathcal{H}$  is used to block the low frequency content of the neural signal, while the low-pass filter eliminates the high frequencies. The  $\mathcal{F}$  matrix is a translational invariant filter to sample the signal as a way of reducing the size of the signal (compression) without overly reducing its information content to process the undulatory motion of locomotion according to its eigenvalues.

Roughly speaking, the filter  $\mathcal{H}$  measures the self-similarity on either side of the center point and the output will be maximal when each the two points are equal to each other. The filter  $\mathcal{F}$  operates on the inputs of the imprimitive systems of the forward circuit. The fact that this matrix appears only in the forward circuit suggests that it might be an important controller in the undulatory motion. This can be seen from the eigenvalues  $\lambda_i$  of this circulant matrix and their eigenvectors  $\mathbf{v}_i$ :

$$\begin{aligned}\lambda_1 &= -2, & \mathbf{v}_1 &= \frac{1}{2}(-1, 1, -1, 1), \\ \lambda_2 &= 2, & \mathbf{v}_2 &= \frac{1}{2}(1, 1, 1, 1), \\ \lambda_3 &= 0, & \mathbf{v}_3 &= \frac{1}{\sqrt{2}}(0, -1, 0, 1), \\ \lambda_4 &= 0, & \mathbf{v}_4 &= \frac{1}{\sqrt{2}}(-1, 0, 1, 0),\end{aligned}\tag{15}$$

which determine the solution of Equation (13) [4] and act by filtering out two modes and allow oscillations between  $\lambda_1$  and  $\lambda_2$ . Thus, the circulant blocks act as information processing units in the recurrent network that are basically filters to perform specific signal processing operations (see Supplementary Note 8).

The association of the circulant processing units with the blocks of imprimitivity completes the operational definition of the locomotor function determined by the decomposition properties of its symmetry group, and in turn, unveil and classify hitherto hidden mechanisms of the neural code. The existence of the predicted blocks can be directly tested in future experiments by measuring how the imprimitive blocks process the neural signal in

real time according to their circulant filters.

### III. DISCUSSION

Overall, the structure-function relation in the connectome can be seen as a refining process of nested symmetry building blocks. The primary building blocks are defined through the mechanism of direct product factorization of normal subgroups and provide a rigorous characterization of the network connectivity structure, and a simple interpretation of its major functions into neural classes. These major sectors are comprised of secondary topological structures involved in signal processing which refine the primary normal subgroups into irreducible blocks of imprimitivity.

The factorization of the symmetry groups of the connectome has its analogy with integers and primes as every integer can be factorized into a unique product of prime numbers as stated in the fundamental theorem of arithmetic. This factorization is also analogous to that of the Standard Model of particle physics [29]. In theoretical physics, automorphisms describe the symmetries of elementary particles and forces [29, 33], as well as atoms, molecules and phases of matter [34]. For example, fundamental forces in particle physics are based on symmetry principles incorporated through a description of the gauge symmetry group of the Lagrangian factorized into three subgroups as  $U(1) \times SU(2) \times SU(3)$ , where  $SU(N)$  is the special unitary group of  $N \times N$  unitary matrices with determinant 1, and  $U(1)$  is the group consisting of all complex numbers with absolute value 1. In this case, each subgroup determines a different force, namely the electroweak and strong forces, and the generators of these symmetry subgroups are the particles. Analogously, the functions of locomotion are based on the symmetries of the connectome through the symmetry group which is factorized in general as  $T \times C \times M$  where each symmetry subgroup determines a different function. For instance, the symmetry group of the chemical forward circuit splits as:  $\mathbf{F}_{\text{ch}} = \mathbf{T}_{\text{F}_{\text{ch}}} \times \mathbf{C}_{\text{F}_{\text{ch}}} \times \mathbf{M}_{\text{F}_{\text{ch}}}$ .

In a milestone in the history of mathematics, all finite simple groups have been discovered and classified into 3 major classes: cyclic, alternating or Lie type plus 26 extra classes of rare sporadic groups [35]. Out this variety, the locomotion connectome contains only cyclic groups. It would be fascinating to discover other naturally occurring simple groups for other functions in different biological networks. Results presented elsewhere indicate

that symmetries extend to the full connectome and also to genetic networks [36], and they are naturally related to neural synchronization. Thus, the principle of symmetry provides a rigorous mathematical characterization of the structural and functional organization of connectomes down to their information-processing units. This hierarchical symmetric architecture may also serve as guidance to design more efficient artificial neural networks inspired by natural systems.

## IV. METHODS

### Circulant and block-circulant matrices in digital signal processing and the connectome

We find that the system of imprimitivity of the locomotion circuits is comprised of a specific type of blocks, which are represented by circulant matrices [13], [https://en.wikipedia.org/wiki/Circulant\\_matrix](https://en.wikipedia.org/wiki/Circulant_matrix).

It is worth noting that there is *a priori* no reason for the occurrence of this specific type of matrices in the system of imprimitivity. That is, a symmetry group may have a system of imprimitivity that is not composed of circulant matrices. Thus, there are two independent results: first, the connectome is broken down into a system of imprimitivity. Second, the imprimitive blocks have the shape of circulant matrices and block circulant matrices.

A circulant matrix  $P_\ell$  of order  $\ell$  is a square matrix of the form [13]:

$$P_\ell = \text{circ}(c_1, c_2, \dots, c_\ell) = \begin{bmatrix} c_1 & c_2 & c_3 & \dots & c_\ell \\ c_\ell & c_1 & c_2 & \dots & c_{\ell-1} \\ \cdot & \cdot & & & \cdot \\ \cdot & \cdot & & & \cdot \\ c_2 & c_3 & c_4 & \dots & c_1 \end{bmatrix}. \quad (16)$$

The elements of each row are the same as those from the previous row, but are shifted one position to the right and wrapped around. The circulant matrix is thus determined by the first row or column and therefore it is denoted by [13]:  $P_\ell = \text{circ}(c_1, c_2, \dots, c_\ell)$ .

We also find block-circulant matrices in the connectome which are defined as follows. Block-circulant matrices are an extension of circulant matrices where the elements  $c_i$  are now replaced by matrices themselves  $A_i$ . Let  $A_1, A_2, \dots, A_m$  be square matrices of order  $n$ . A block-circulant matrix of order  $mn$  is the form [13]:

$$\mathcal{BC} = \text{bcirc}(A_1, A_2, \dots, A_m) = \begin{bmatrix} A_1 & A_2 & A_3 & \dots & A_m \\ A_m & A_1 & A_2 & \dots & A_{m-1} \\ \cdot & \cdot & & & \cdot \\ \cdot & \cdot & & & \cdot \\ A_2 & A_3 & A_4 & \dots & A_1 \end{bmatrix}, \quad (17)$$

and when  $n = 1$ , the block-circulant becomes a circulant matrix. The matrices  $A_i$  may not

need to be necessarily circulant. However, the connectome presents only circulant matrices as  $A_i$ , thus creating a hierarchical nested structure of circulant blocks made of circulant matrices themselves.

The graph that results from a circulant matrix is called a circulant graph, [https://en.wikipedia.org/wiki/Circulant\\_graph](https://en.wikipedia.org/wiki/Circulant_graph). Circulant matrices are determined by the first row and every row is the cyclic shift of the row above it. A circulant matrix is a special kind of Toeplitz matrix with the additional property that  $c_i = c_{i+\ell}$  [13].

Repeated application of  $P_\ell$  on itself generates an abelian group called **cyclic group** of order  $\ell$ , denoted as  $\mathbf{C}_\ell$ . Moreover, any subgroup of  $\mathbf{C}_\ell$  is also cyclic. The important point is that whenever the symmetry group of a network contains a circulant permutation matrix like  $P_\ell$  in Equation (16), then the adjacency matrix  $A$ , or a piece of it, inherits from  $P_\ell$  the same circulant structure.

In the locomotion neural circuits studied in this work, we find 3 types of circulant matrices:  $\mathcal{H}$ ,  $\mathcal{L}$ , and  $\mathcal{F}$ . In the language of signal processing, the matrix  $\mathcal{H}$  is a spatial high-pass filter, used to block the low frequency content of the signal; and  $\mathcal{L}$  is a spatial low-pass filter, which instead eliminates the high frequencies. These are the two most common linear filters used in image processing. The filter  $\mathcal{F}$  is the kernel of the fast Fourier transform (see Supplementary Note 8). It can be thought as a translational invariant filter to sample the signal as a way of reducing the size of the signal without overly reducing its information content. While  $\mathcal{H}$  and  $\mathcal{L}$  appear consistently across all circuits, the circulant  $\mathcal{F}$  matrix occurs only in the forward gap-junction circuit. The low pass filter selects the ‘bulk’ of the information, while the ‘high-pass’ picks out finer details.

This structure shows how the connectome acts as a signal processing network within a hierarchical structure that starts at the symmetry group level, which is then broken down into subgroups and further broken into the system of imprimitivity which represents the irreducible building blocks.

**Data availability:** Connectome data are available in the public domain at <http://www.wormatlas.org> and codes at <http://www.kcorelab.org> and <http://github.com/Makselab>.

- 
- [1] Hartwell, L. H., Hopfield, J. J., Leibler, S. & Murray, A. W. From molecular to modular cell biology. *Nature* **402**, C47-C52 (1999).
- [2] Buchanan, M., Caldarelli, G., De Los Rios, P., Rao, F. & Vendruscolo, M. (editors), *Networks in Cell Biology* (Cambridge University Press, Cambridge, 2010).
- [3] Alon, U. *An Introduction to Systems Biology: Design Principles of Biological Circuits* (CRC Press, Boca Raton, 2006).
- [4] Dayan, P. & Abbott, L. F. *Theoretical Neuroscience: Computational and Mathematical Modeling of Neural Systems* (The MIT Press, Cambridge, 2001).
- [5] White, J. G., Southgate, E., Thomson, J. N. & Brenner, S. The structure of the nervous system of the nematode *Caenorhabditis elegans*. *Philos. Trans. R. Soc. Lond. B* **314**, 1-340 (1986).
- [6] Chalfie, M. *et al.* The neural circuit for touch sensitivity in *Caenorhabditis elegans*. *J. Neurosci.* **5**, 956-964 (1985).
- [7] Gray, J. M., Hill, J. J. & Bargmann, C. I. A circuit for navigation in *Caenorhabditis elegans*. *Proc. Acad. Sci. US* **102**, 3184-3191 (2005).
- [8] Chen, B. L., Hall, D. H. & Chklovskii, D. B. Wiring optimization can relate neuronal structure and function. *Proc. Nat. Acad. US* **103**, 4723-4728 (2006).
- [9] Varshney, L. R., Chen, B. L., Paniagua, E., Hall, D. H. & Chklovskii, D. B. Structural properties of the *Caenorhabditis elegans* neuronal network. *PLoS Comput. Biol.* **7**, e1001066 (2011).
- [10] Kato, S., Kaplan, H. S., Schrödel, T., Skora, S., Lindsay, T. H., Yemini E., Lockery, S. & Zimmer, M. Global brain dynamics embed the motor command sequence of *Caenorhabditis elegans*. *Cell* **163**, 656-669 (2015).
- [11] Yan, G., Vértès, P. E., Towilson, E. K., Chew, Y. L., Walker, D. S., Schafer, W. R. & Barabási, A.-L. Network control principles predict neuron function in the *Caenorhabditis elegans* connectome. *Nature* **550**, 519-523 (2017).
- [12] Dixon, J. D. & Mortimer, B. *Permutation Groups*, Graduate Texts in Mathematics, 163 (Springer-Verlag, New York, 1996).
- [13] Gray, R. M. *Toeplitz and Circulant Matrices: A Review*, Foundation and Trends in Communi-



- cations and Information Theory, vol 2, no 3, pp. 155-239 (2006). [https://www.ic.tu-berlin.de/fileadmin/fg121/Source-Coding\\_WS12/selected-readings/Gray\\_\\_2005.pdf](https://www.ic.tu-berlin.de/fileadmin/fg121/Source-Coding_WS12/selected-readings/Gray__2005.pdf)
- [14] Golubitsky, M. & Stewart, I. Nonlinear dynamics of networks: the groupoid formalism, *Bull. Amer. Math. Soc.* **43**, 305-364 (2006).
  - [15] Pecora, L. M. Sorrentino, F., Hagerstrom, A. M., Murphy, T. E. & Roy, R. Cluster synchronization and isolated desynchronization in complex networks with symmetries. *Nature Comm.* **5**, 4079 (2014).
  - [16] Durbin, R. M. Studies on the development and organisation of the nervous system of *Caenorhabditis elegans*. [PhD thesis], University of Cambridge (1987).
  - [17] Hall, D. H. & Russell, R. L. The posterior nervous system of the nematode *Caenorhabditis elegans*: serial reconstruction of identified neurons and complete pattern of synaptic interactions. *J. Neurosci.* **11**, 1-22 (1991).
  - [18] Chalfie, M. & White, J. The Nervous System, in *The nematode Caenorhabditis elegans*, edited by Wood, W. B. and the Community of *C. elegans* Researchers (Cold Spring Harbor Laboratory Press, 1988). <https://www.ncbi.nlm.nih.gov/books/NBK19982/figure/A783/>.
  - [19] Zhen, M. & Samuel, A. D. T. *C. elegans* locomotion: small circuits, complex functions. *Cur. Opinion Neurobiol.* **33**, 117-126 (2015).
  - [20] Nguyen, J., P., Shipley, F. B., Linder, A. N, Plummer, G. S., Liu, M., Setru, S. U., Shaevitz, J. W. & Leifer, A. M. Whole-brain calcium imaging with cellular resolution in freely behaving *Caenorhabditis elegans*. *Proc. Natl. Acad. Sci. USA* **113**, E1074-E1081 (2016).
  - [21] Sorrentino, F., Pecora, L. M., Hagerstrom, A. M., Murphy, T. E. & Roy, R. Complete characterization of the stability of cluster synchronization in complex dynamical networks. *Science Adv.* **2**, e1501737 (2016).
  - [22] Abrams, D. M., Pecora, L. M. & Motter, A. E. Focus issue: Patterns of network synchronization. *Chaos* **26**, 094601 (2016).
  - [23] Giles, A. C., Rose, J. K. & Rankin, C. H. Investigations of learning and memory in *Caenorhabditis elegans*. *Int. Rev. Neurobiol.* **69**, 37-71 (2005).
  - [24] Tao, T. *Topics in Random Matrix Theory*, Graduate Studies in Mathematics, Volume **132**. American Mathematical Society (2012).
  - [25] Altun, Z. F. & Hall, D. H. Wormatlas. (2002-2006). Available: <http://www.wormatlas.org>.
  - [26] Tononi, G., Sporns, O. & Edelman, G. M. A measure for brain complexity: relating functional

- segregation and integration in the nervous system. *Proc. Nat. Acad. Sci. USA* **91**, 5033-5037 (1994).
- [27] Girvan, M. & Newman, M. E. J. Community structure in social and biological networks. *Proc. Nat. Acad. Sci. US* **99**, 7821-7826 (2002).
- [28] Blondel, V. D., Guillaume, J.-L., Lambiotte, R. & Lefebvre, E. Fast unfolding of communities in large networks. *J. Stat. Mech.: Theory and Experiment* **10** P1000 (2008).
- [29] Weinberg, S. *The Quantum Theory of Fields* (Cambridge University Press, Cambridge, 2005).
- [30] Mitra, A. K. & Kuo, Y. *Digital Signal Processing: a Computer-based Approach* (McGraw-Hill, 2006).
- [31] Henriques, J. F., Caseiro, R., Martins, P. & Batista, J. Exploiting the Circulant Structure of Tracking-by-Detection with Kernels. In: Fitzgibbon A., Lazebnik S., Perona P., Sato Y. & Schmid C. (eds) *Computer Vision - ECCV 2012. Lecture Notes in Computer Science*, Vol **7575**. Springer, Berlin, Heidelberg pp. 702-715 (2012).
- [32] Mathieu, M., Henaff, M. & LeCun, Y. Fast training of convolutional networks through FFTs. International Conference on Learning Representations (ICLR2014), CBLS, April 2014. <https://arxiv.org/abs/1312.5851>
- [33] Georgi, H. *Lie Algebras in Particle Physics: from Isospin to Unified Theories*. Frontier in Physics, Vol 54 (Westview Press, 2nd edn, 1999).
- [34] Landau, L. D. & Lifshitz, E. M. *Quantum Mechanics: Non-Relativistic Theory (Volume 3)*, third edition (Butterworth-Heinemann, Oxford, 1977). Ch. XII and Ch. XIII explain symmetries in atoms and molecules.
- [35] Gorenstein, D. The classification of finite simple groups. Vol. 1. Groups of noncharacteristic 2 type, The University Series in Mathematics (Plenum Press, 1983).
- [36] Morone, F., Leifer, I. & Makse, H. A. Fibration building blocks of information-processing networks. Preprint at <https://bit.ly/2Z94B6o> (2019).
- [37] McKay, B. D. Nauty users guide (version 1.5), Tech. Rep. TR-CS-90-02, Australian National University (1990).

**Acknowledgments:** We are grateful to L. Parra, A. Holodny, and I. Leifer for discussions. This work was supported by grants from NIH-NIBIB R01EB022720, NIH-NCI

**Authors contributions:** F.M. and H.A.M. contributed equally to this work.

**Competing interests:** Authors have no competing interests.

**FIG. 1. Group theoretical definitions: automorphism, symmetry groups, pseudosymmetries, normal subgroups, and blocks of imprimitivity.** (a) Circuit made of gap-junction and only interneurons in the forward locomotion used to define an automorphism. These are permutation symmetries that leave the adjacency structure invariant. These symmetries then convert to a system of imprimitivity when we integrate the circuit into the full locomotion connectome. Nodes represent neurons and weighted links represent the number of gap-junctions connections between neurons from Ref. [9]. (b) Adjacency matrix of the circuit in (a). This matrix is composed of circulant matrices: a high-pass filter  $\mathcal{H} = \text{circ}(0, 1)$  in the diagonal and an off-diagonal low-pass filter  $\mathcal{L} = \text{circ}(1, 1)$ . The full  $4 \times 4$  matrix forms a block-circulant matrix  $\mathcal{BC} = \text{bcirc}(\mathcal{H}, \mathcal{L})$  [13] (see Methods Section for definitions). (c) Symmetry group of the circuit shown in (a), called dihedral group  $\mathbf{D}_8$ , comprises 8 automorphisms out of the  $4! = 24$  possible permutations of neurons. We show each permutation matrix  $P$  of each automorphism. (d) Pseudosymmetries capture inherent variabilities in the connectome from animal to animal. An example pseudosymmetry is shown  $P_\varepsilon = \text{DB5} \leftrightarrow \text{DB6}$  that breaks one link to AVBR over 18 total weighted links, giving  $\varepsilon = 1/18 = 5.5\%$ . (e) Definition of normal subgroup. A subgroup  $\mathbf{H}$  is said to be normal in a group  $\mathbf{G}$  if and only if  $\mathbf{H}$  commutes with every element  $g \in \mathbf{G}$ , that is:  $[g, \mathbf{H}] = g\mathbf{H} - \mathbf{H}g = 0$  (see Supplementary Note 4 for a detailed explanation). (f) Definition of blocks of imprimitivity and system of imprimitivity. Simply put, a set of nodes is called a block (of imprimitivity) if all nodes in this set always ‘move together’ under any automorphism of the symmetry group. A set of blocks with such a property is thus called a system of imprimitivity (see Supplementary Note 7 for a formal definition). (g) Definition of circulant matrix and circular convolution. Matrix  $\mathcal{F}$  appears in the forward gap-junction locomotion circuit and is called a circulant matrix. This matrix has a peculiar pattern where each row is a shift to the right by one entry of the previous row. Multiplication of  $\mathcal{F}$  by a vector  $\mathbf{x}$  gives rise to a famous operation called a circular convolution, which is used in many applications, ranging from digital signal processing, image compression, and cryptography

to number theory, theoretical physics and engineering, often in connection with discrete and fast Fourier transforms, as explained in Supplementary Note 8.

FIG. 2. **Symmetry group  $F_{\text{gap}}$  of the forward gap-junction circuit.** (a) Circuit from Ref. [9]. Pseudosymmetries  $P_\varepsilon$  act on distinct sectors of neurons indicated by different colors that lead to direct product factorization of the symmetry group into normal subgroups. The normal subgroups sectors of neurons match the broad classification of command interneurons and motor neurons from the Wormatlas [25]. (b) Adjacency matrix of (a) showing the normal subgroup structure and its matching with broad neuronal classes. (c) Idealization of the circuit obtained from (a) by  $\varepsilon \rightarrow 0$  leading to perfect symmetries (see Supplementary Note 3). We highlight the two 4-cycles across  $\mathcal{B}_1$ :  $\text{VB2} \rightarrow \text{DB3} \rightarrow \text{DB2} \rightarrow \text{VB1} \rightarrow \text{VB2}$  and its conjugate  $\mathcal{B}_2$ :  $\text{DB1} \rightarrow \text{VB4} \rightarrow \text{VB5} \rightarrow \text{VB6} \rightarrow \text{VB4}$  that give rise to the circulant matrix structure highlighted in the checker-board pattern in (d) of both imprimitive blocks. (d) Adjacency matrix of the ideal circuit in (c). We highlight the two imprimitive blocks  $\mathcal{B}_1 = (\text{VB2}, \text{DB3}, \text{DB2}, \text{VB1})$  and  $\mathcal{B}_2 = (\text{DB1}, \text{VB4}, \text{VB5}, \text{VB6})$  mentioned in the text and its circulant structure in the normal subgroup  $\mathbf{D}_1$ . The other normal subgroups are also described by circulant blocks and correspond to imprimitive blocks:  $\mathcal{B}_3, \mathcal{B}_4, \mathcal{B}_5, \mathcal{B}_6, \mathcal{B}_7$ , as indicated. Some of these structures also form block-circulant matrices. Each block of the adjacency matrix  $A$  performs a fundamental signal processing task.

FIG. 3. **Symmetry group  $B_{\text{gap}}$  of the backward gap-junction circuit.** (a) The real circuits and (b) its adjacency matrix. The symmetry group is factorized as a direct product of normal subgroups:  $B_{\text{gap}} = [\mathbf{C}_2 \times \mathbf{C}_2 \times \mathbf{D}_1] \times [\mathbf{S}_{12} \times \mathbf{D}_6 \times \mathbf{C}_2]$ , which leads to a partition of neurons in two sectors that match the command and motor sectors known experimentally, as indicated. (c) Ideal circuit and (d) adjacency matrix highlighting the primitive and imprimitive blocks and their circulant structures from  $\mathcal{B}_1$  to  $\mathcal{B}_9$ .

FIG. 4. **Symmetry groups  $F_{\text{ch}}$  and  $B_{\text{ch}}$  of the chemical synapse forward and backward circuits.** (a) Forward locomotor chemical synapse circuit and (b) its adjacency matrix (ideal circuits, real circuits in Supplementary Figs 5 and 6). The symmetry group  $F_{\text{ch}}$  is factorized into the direct product of command, motor, and touch subgroups as  $F_{\text{ch}} = \mathbf{C}_2 \times [\mathbf{D}_1] \times [\mathbf{S}_{10} \times \mathbf{D}_1]$ , which, in turn, split up the circuits into independent sectors of neurons matching different functions and include also the neuron touch class PVC (forward)

and AVD (backward). **(c)** The backward circuit factorizes as  $\mathbf{B}_{\text{ch}} = \mathbf{C}_2 \times [\mathbf{C}_2 \times \mathbf{C}_2] \times [\mathbf{S}_5 \times \mathbf{S}_4 \times \mathbf{S}_3 \times \mathbf{D}_1 \times \mathbf{C}_2 \times \mathbf{C}_2]$ . We show the ideal circuit and **(d)** its adjacency matrix. For simplicity we plot only the interneurons that connect to the motor neurons. Full circuit in SM Fig. 6. All neurotransmitters are cholinergic and excitatory (ACh) except for RIM which uses neurotransmitter Glutamate and Tyramine and AIB which is glutamatergic (see Supplementary Note 6). These different types of synaptic interactions respect the symmetries of the circuits, see Supplementary Note 5.

**FIG. 5. Symmetry vs other methods.** We compare the functional classes obtained from symmetries with modularity detection algorithms [27, 28] and a typical eigenvector centrality measure. **(a)** Forward gap-junction circuit classes obtained using modularity or community detection detection algorithm from [28] and **(b)** using eigenvector centrality. **(c)** Backward gap-junction circuit modularity and **(d)** eigenvector centrality. Both measures, modular detection and centrality, do not capture the symmetries and functional classification of this connectome.

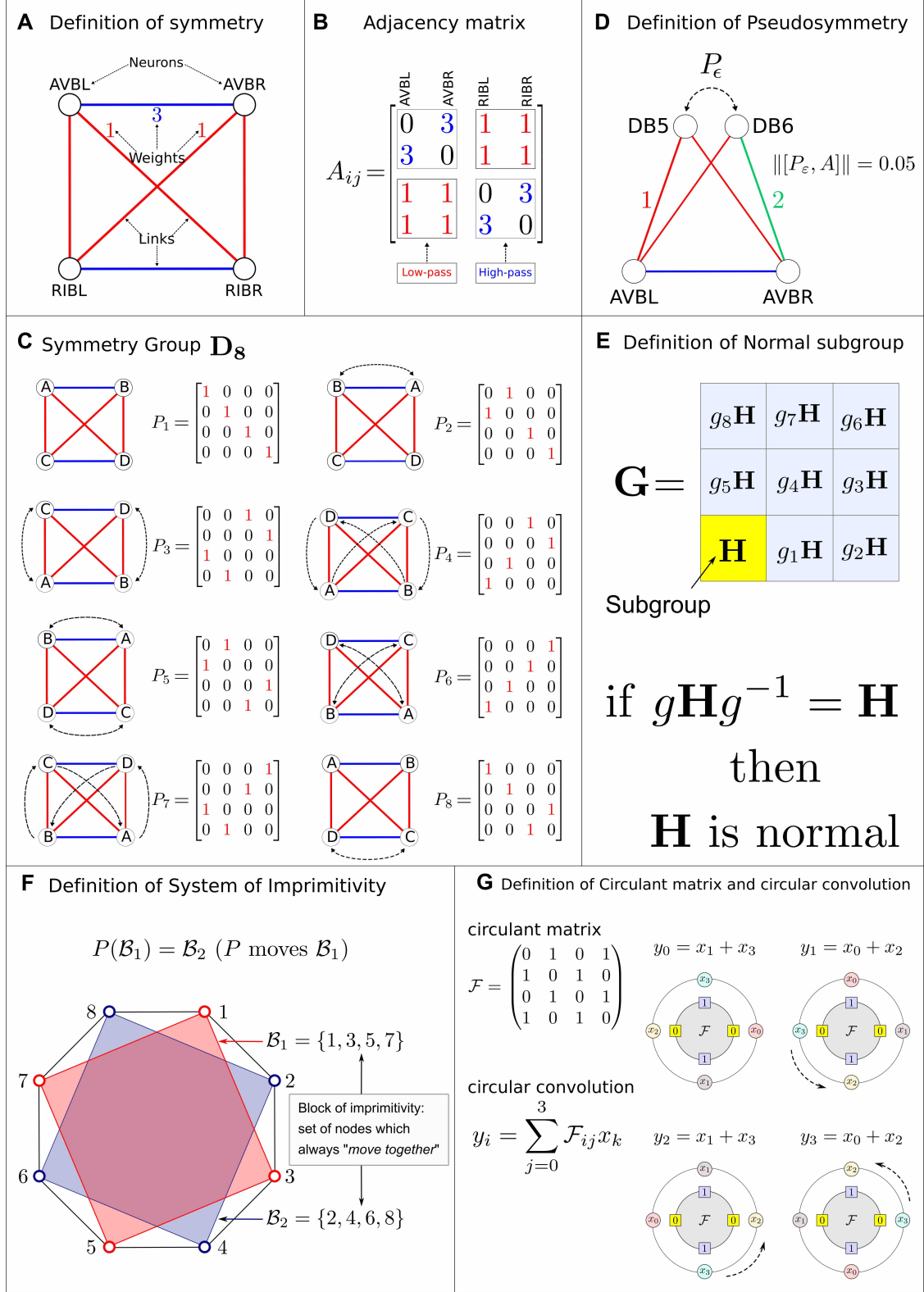
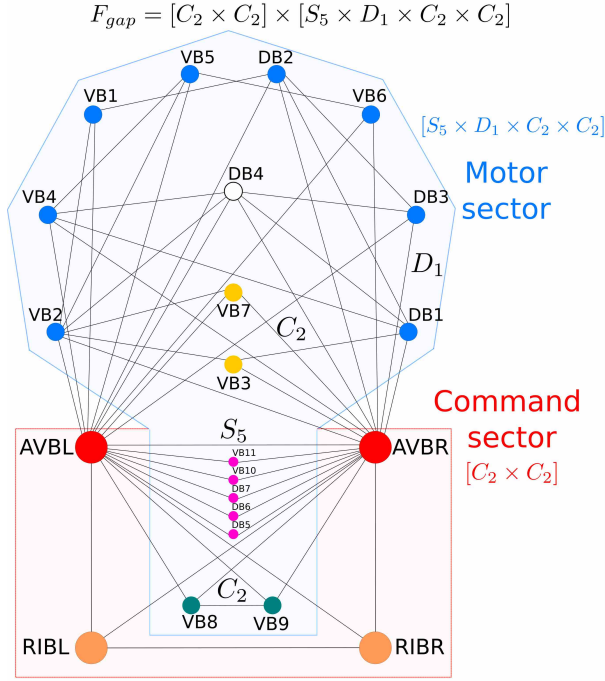
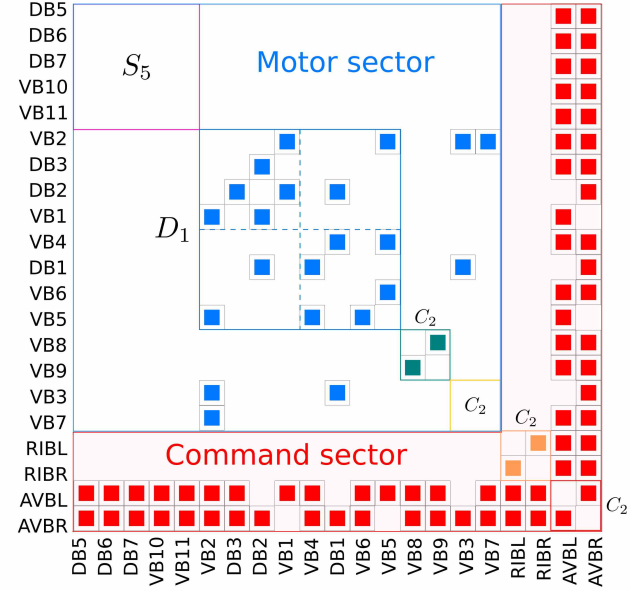


FIG. 1.

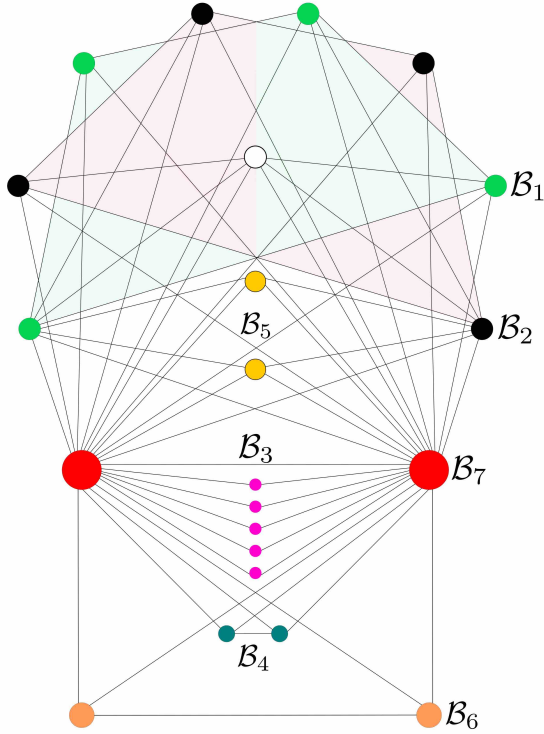
### A Forward gap-junction circuit



### B Adjacency Matrix. Real circuit



### C System of imprimitivity Circulant block



### D Adjacency Matrix. Ideal circuit

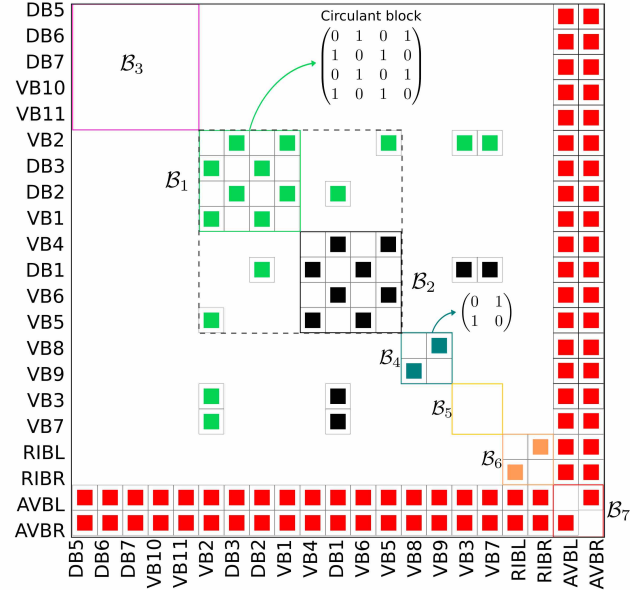
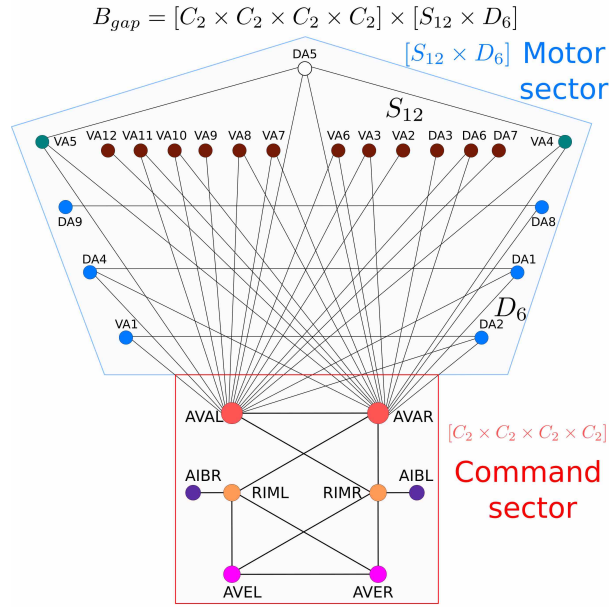
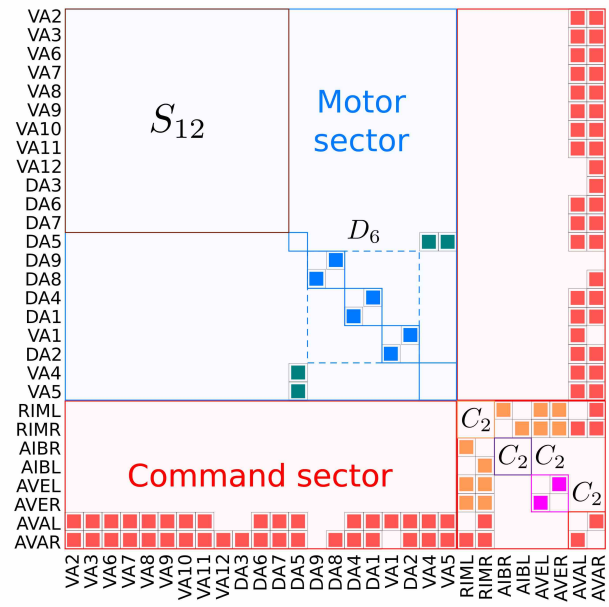


FIG. 2.

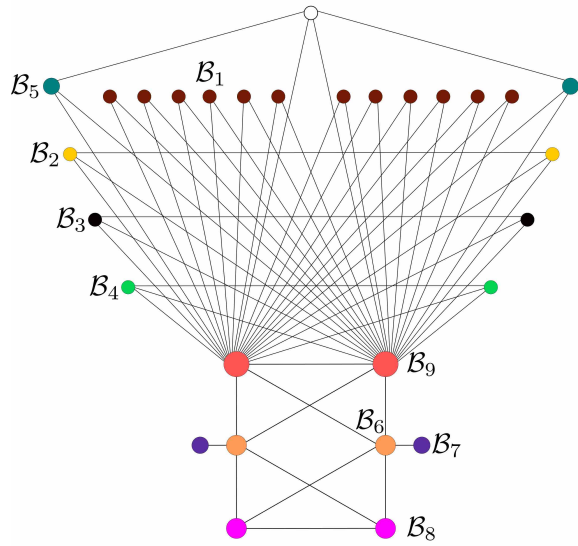
### A Backward gap-junction circuit



### B Adjacency matrix. Real circuit



### C System of imprimitivity Circulant block



### D Adjacency matrix. Ideal circuit

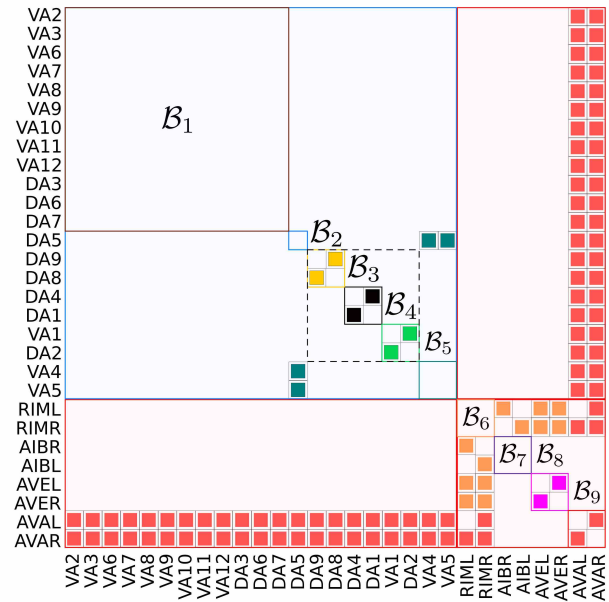
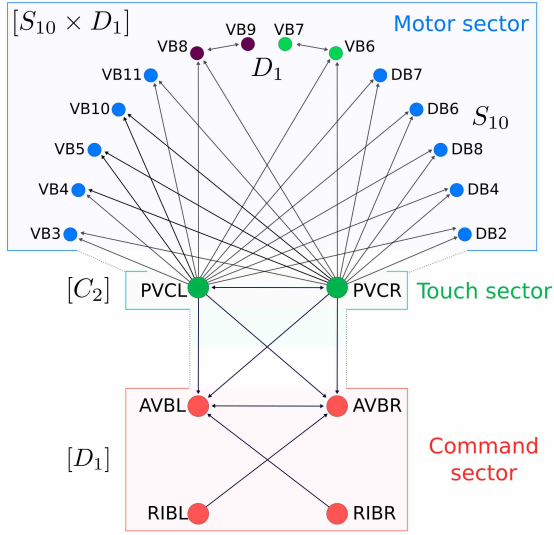


FIG. 3.



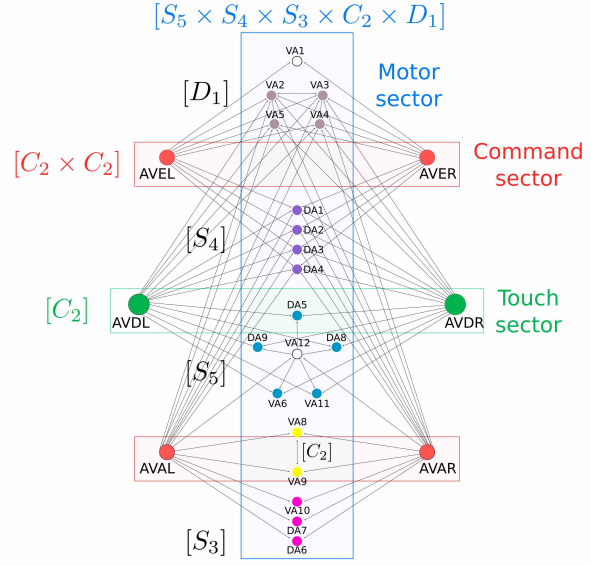
**A** Forward chemical synapse circuit

$$F_{ch} = [C_2] \times [D_1] \times [S_{10} \times D_1]$$

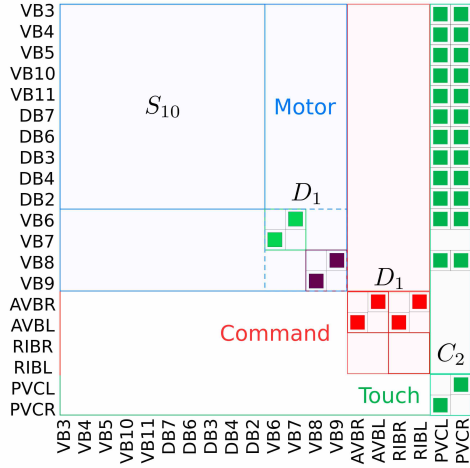


**C** Backward chemical synapse circuit

$$B_{ch} = [C_2] \times [C_2 \times C_2] \times [S_5 \times S_4 \times S_3 \times C_2 \times D_1]$$



**B** Adjacency matrix. Circulant block



**D** Adjacency matrix. Circulant block

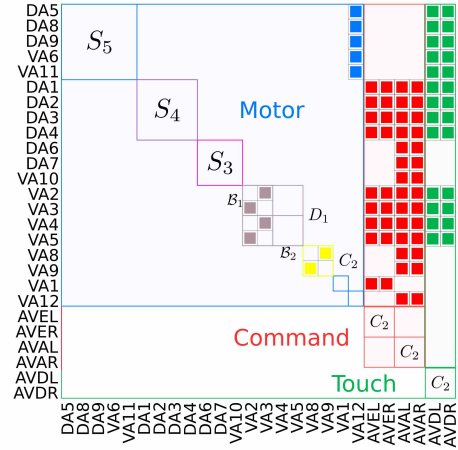
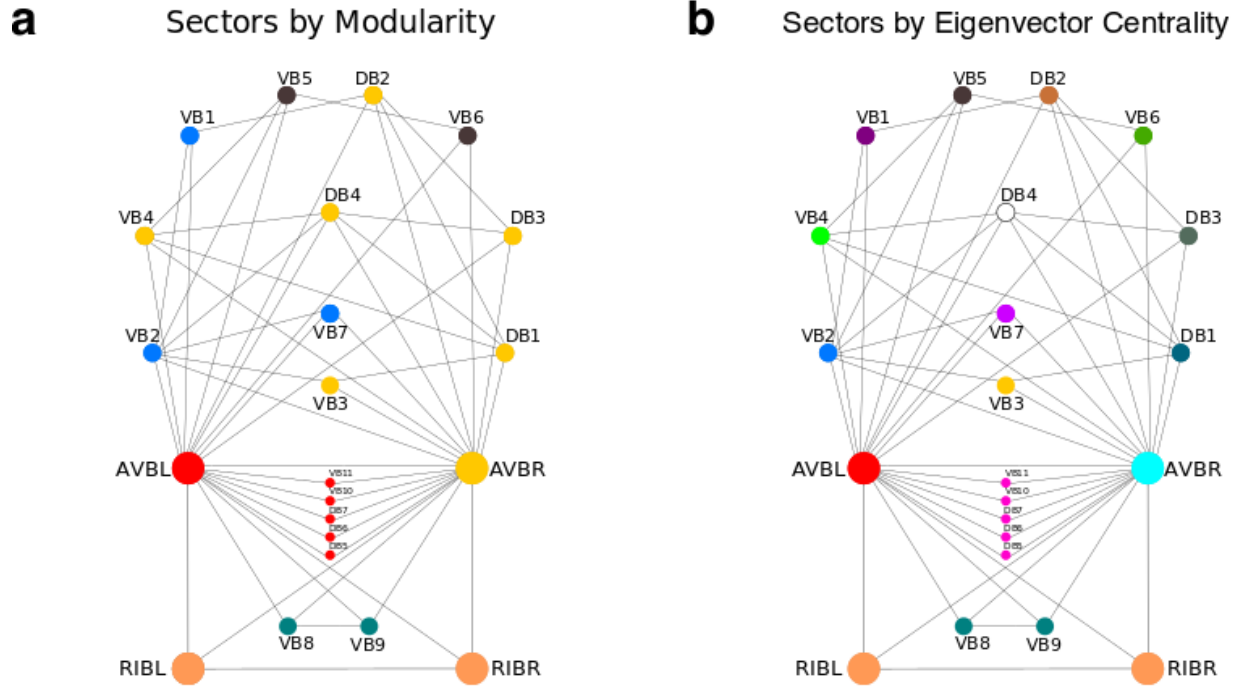


FIG. 4.

## Forward gap-junction circuit



## Backward gap-junction circuit

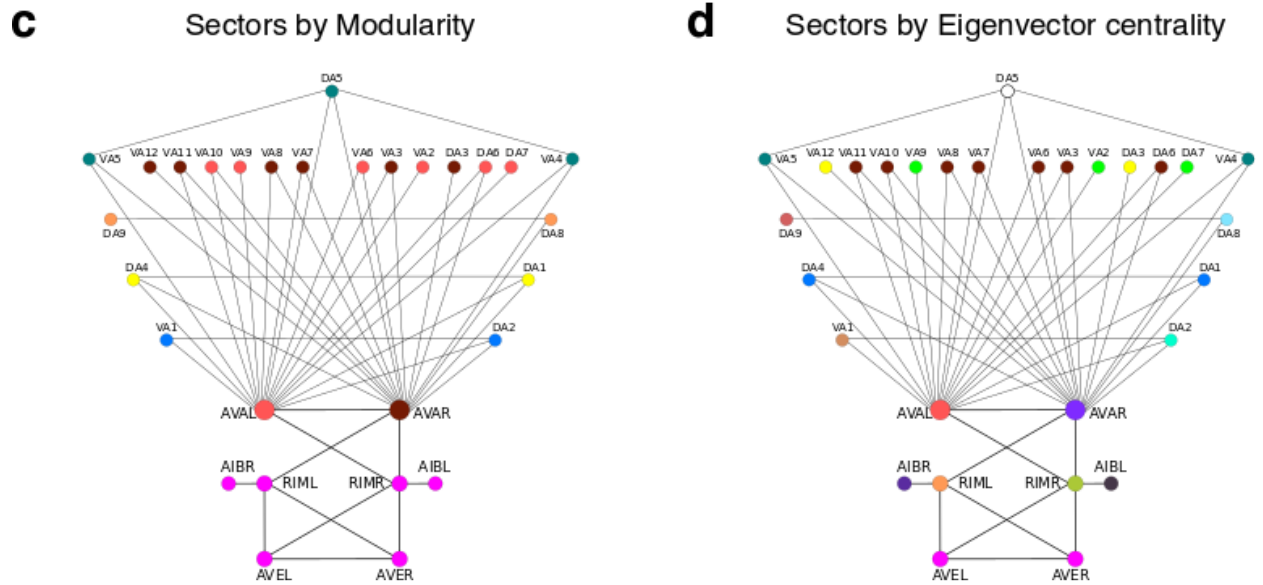


FIG. 5.

| <b>Pseudosymmetry - Forward gap-junction</b>                    | $\varepsilon$ (%) | Subgroup              | p-value            |
|---|-------------------|-----------------------|--------------------|
| (RIBL, RIBR)  | 0.0%              | <b>C<sub>2</sub></b>  | 0.001              |
| (VB3, VB7)  | 5.3%              | <b>C<sub>2</sub></b>  | 0.02               |
| (VB8, VB9)  | 9.6 %             | <b>C<sub>2</sub></b>  | 0.004              |
| (AVBL, AVBR)  | 24.5%             | <b>C<sub>2</sub></b>  | 0.0007             |
| (DB5, DB6, DB7, VB10, VB11)                                     | 5.5 %             | <b>S<sub>5</sub></b>  | 0.0002             |
| (DB1, VB2, DB2, VB5, DB3, VB4, VB1, VB6)                        | 23.4%             | <b>D<sub>1</sub></b>  | 0.00001            |
| <b>Pseudosymmetry - Backward gap-junction</b>                   | $\varepsilon$ (%) | Subgroup              | p-value            |
| (AIBL, AIBR, RIML, RIMR)  | 1.5%              | <b>D<sub>1</sub></b>  | 0.00001            |
| (DA8, DA9, DA2, VA1, DA1, DA4 )                                 | 6.9%              | <b>D<sub>6</sub></b>  | $< 10^{-6}$        |
| (AVEL, AVER)  | 1.5%              | <b>C<sub>2</sub></b>  | 0.005              |
| (VA4, VA5)  | 3.8%              | <b>C<sub>2</sub></b>  | 0.005              |
| (VA2, VA3, VA6, VA7, VA8, VA9, VA10, VA11, VA12, DA3, DA6, DA7) | 13.8%             | <b>S<sub>12</sub></b> | $< 10^{-6}$        |
| <b>Pseudosymmetry - Forward chemical synapse</b>                | $\varepsilon$ (%) | Subgroup              | p-value            |
| (VB3, VB4, VB5, VB10, VB11, DB2, DB4, DB6, DB7, DB8)            | 3.8%              | <b>S<sub>10</sub></b> | 0.014              |
| (VB6, VB7, VB8, VB9)  | 3.8%              | <b>D<sub>1</sub></b>  | 0.0012             |
| (PVCL, PVCR)  | 3.8%              | <b>C<sub>2</sub></b>  | 0.0006             |
| (AVBL, AVBR, RIBL, RIBR )                                       | 7.6%              | <b>D<sub>1</sub></b>  | $< 10^{-6}$        |
| <b>Pseudosymmetry - Backward chemical synapse</b>               | $\varepsilon$ (%) | Subgroup              | p-value            |
| (VA2, VA3, VA4, VA5)  | 4.5%              | <b>D<sub>1</sub></b>  | 0.002              |
| (VA8, VA9)  | 0.8%              | <b>C<sub>2</sub></b>  | $9 \times 10^{-5}$ |
| (DA5, DA8, DA9, VA6, VA11)                                      | 10.8%             | <b>S<sub>5</sub></b>  | $< 10^{-6}$        |
| (AVAL, AVAR)  | 21.5%             | <b>C<sub>2</sub></b>  | $4 \times 10^{-6}$ |
| (AVEL, AVER)  | 15.5%             | <b>C<sub>2</sub></b>  | $8 \times 10^{-5}$ |
| (AVDL, AVDR)  | 24.5%             | <b>C<sub>2</sub></b>  | 0.004              |
| (DA1, DA2, DA3, DA4)  | 2.3%              | <b>S<sub>4</sub></b>  | $4 \times 10^{-6}$ |
| (VA10, DA6, DA7)  | 3.8%              | <b>S<sub>3</sub></b>  | 0.002              |

TABLE I. Pseudosymmetries of the locomotion circuit. For each subgroup we show the uncertainty constant  $\varepsilon$ , which is below the 25% uncertainty given by the animal to animal experimental variability, and therefore the pseudosymmetries have biological significance. The provided p-value indicates that the pseudosymmetries have also statistical significance.

## Supplementary Information

### Symmetry group factorization reveals the structure-function relation in the neural connectome of *Caenorhabditis elegans*

Flaviano Morone and Hernán A. Makse

#### Supplementary Note 1 - *C. elegans* connectome

We downloaded the most updated connectome of the hermaphrodite worm *Caenorhabditis elegans* (*C. elegans*) from the curated database of Varshney *et al.* [9] which is freely available through the Wormatlas: Altun, Z. F., Hall, D. H. (2002-2006) Wormatlas [25]. Available: <http://www.wormatlas.org>. Varshney *et al.* report a wiring diagram based on the original data from White *et al.* [5] augmented to include new serial section electron microscopy reconstructions. The connectome is composed of gap junctions which provide direct electrical couplings between neurons and therefore represent undirected (bidirectional) links between neurons. It is also composed of chemical synapses which use neurotransmitters to transmit signals at the synaptic cleft from a neuron to a target neuron and are therefore represented by directed links in the circuits. Here we consider the circuits of interneurons and motor neurons involved in two locomotion functions: forward and backward locomotion. The interneurons connect to motor neurons of classes A and B that control body wall muscles [5, 6, 19]. All neurons studied here are cholinergic and excitatory (ACh) except for RIM which uses neurotransmitter Glutamate and Tyramine and AIB which is glutamatergic (see Supplementary Note 6). The different types of synaptic interactions respect the symmetries found in the circuits.

#### Supplementary Note 2 - Network symmetry group

A network is a set of nodes  $V = \{1, \dots, N\}$  endowed with a connectivity structure defined by a set of edges  $E$  between pair of nodes. An edge  $i \rightarrow j$  is interpreted as an arrow directed from node  $i$  to node  $j$ , which are said to be connected (or adjacent) to one another. The connectivity structure defined by the edge-set  $E$  can be put into the  $N \times N$  adjacency matrix  $A$ , which has nonzero entries  $A_{ij} \neq 0$  only if there is an edge  $i \rightarrow j \in E$  connecting nodes  $i$  to  $j$ , and  $A_{ij} = 0$  otherwise. We consider a weighted adjacency matrix to take into account the number of synaptic connections as given by [9].

The concept of permutation is as follows. A permutation of a network, denoted as  $P$ , is a bijective map  $P : V \rightarrow V$  which pairs each node  $i \in V$  with exactly one node  $P(i) \in V$ , and there are no unpaired nodes (whence the term bijective map). As a consequence, any permutation  $P$  has always a well-defined inverse, denoted as  $P^{-1}$ . Moreover, since permutations are orthogonal transformation, we have that  $P^{-1} = P^T$ , where  $P^T$  denotes the matrix transpose. Two permutations  $P_1$  and  $P_2$  can be composed (or multiplied), the result being another permutation. Composition of two permutations is written as  $P_1 \circ P_2$ , and the operation denoted by  $\circ$  is called *composition law*. In the following, we omit for simplicity the symbol  $\circ$  and write the composition as  $P_1 \circ P_2 \equiv P_1 P_2$ .

A set of permutations  $\mathbf{G} = \{P_1, \dots, P_n\}$  is said to form a **permutation group** under composition of its elements if it obeys the group axioms [12] listed below. **Definition of Permutation Group:**

1. existence of the **identity**  $I \in \mathbf{G}$ , defined as  $I(i) = i$  for all  $i$ .
2. **associativity** of the composition law :  $P_i(P_j P_k) = (P_i P_j) P_k$ ;
3. **closure** of the composition law:  $P_i P_j \in \mathbf{G}$ ;
4. existence of the **inverse**  $P_i^{-1}$  for all  $P_i \in \mathbf{G}$ , defined by  $P_i^{-1} P_i = P_i P_i^{-1} = I$ .

In a network of size  $N$  there are  $N!$  different ways to permute its nodes. The set of these  $N!$  permutations obeys the group axioms listed above, so it forms a group. However, this is not the symmetry group of the network, because not all permutations are, in general, symmetries. To qualify as a network symmetry,  $P$  must preserve the connectivity structure, i.e., the network adjacency matrix  $A$  [12, 15, 21, 22]. In other words, the permuted adjacency matrix  $PAP^{-1}$  must be identical to the original one:  $A = PAP^{-1}$  if  $P$  is a permutation symmetry. Invariance of  $A$  under  $P$  is formally equivalent to the requirement that  $P$  commutes with  $A$ , so we have the formal definition of symmetry:

$$[P, A] \equiv PA - AP = 0 \quad \Longleftrightarrow \quad P \text{ is a permutation symmetry} . \quad (18)$$

Permutations which obey Eq. (18) are formally called network automorphisms [12]. In short, network symmetry and automorphism are synonyms of one another. For example, consider the circuit shown in Supplementary Fig. 1a, and the permutation  $P$  acting on it represented

by the matrix

$$P = \begin{matrix} \text{AVBL} \\ \text{AVBR} \\ \text{RIBL} \\ \text{RIBR} \end{matrix} \begin{pmatrix} 0 & 0 & 1 & 0 \\ 0 & 0 & 0 & 1 \\ 1 & 0 & 0 & 0 \\ 0 & 1 & 0 & 0 \end{pmatrix}, \quad (19)$$

which swaps AVBL with RIBL, and AVBR with RIBR. This permutation is an automorphism, because the circuits before and after the action of  $P$  are exactly the same, as seen in Supplementary Fig. 1a. Moreover, it is easy to check that  $[P, A] = 0$ . Next, consider the action of the permutation  $Q$  shown in Supplementary Fig. 1b, given by the matrix

$$Q = \begin{matrix} \text{AVBL} \\ \text{AVBR} \\ \text{RIBL} \\ \text{RIBR} \end{matrix} \begin{pmatrix} 0 & 0 & 0 & 1 \\ 0 & 1 & 0 & 0 \\ 0 & 0 & 1 & 0 \\ 1 & 0 & 0 & 0 \end{pmatrix}, \quad (20)$$

which exchanges AVBL with RIBR and leaves the other neurons fixed. Permutation  $Q$  is not an automorphism, because it does not preserve the connectivity between neurons. Indeed, before the action of  $Q$ , AVBL and AVBR are connected by a link with a weight=3, while after they are connected by a link with a weight=1. Thus,  $Q$  is not a symmetry, because it alters the connectivity structure of the circuit by changing the weights on the links. Consistently, we also have that  $[Q, A] \neq 0$ .

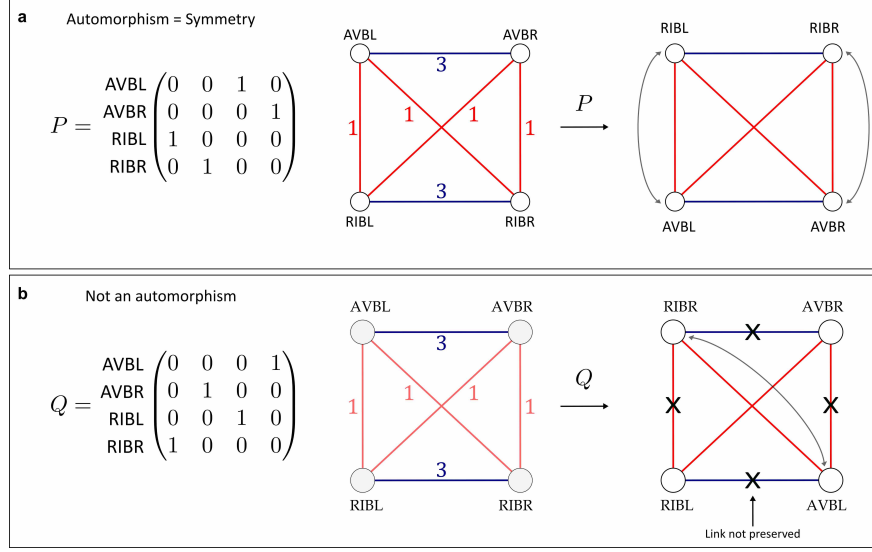
The set of all network automorphisms obeys all group axioms, so it forms a group. This group, denoted as  $\mathbf{G}_{\text{sym}}(A)$ , is called the **permutation symmetry group of the network** [12], and formally defined as:

$$\mathbf{G}_{\text{sym}}(A) = \{P : [P, A] = 0\}. \quad (21)$$

An algorithm to find perfect automorphisms of a given network is call Nauty, and it is given in Ref. [37], which is based on the well-known problem of testing isomorphism of graphs.

### Supplementary Note 3 - Pseudosymmetries

A 25% variation across animals has been found in the connectivity of connectomes [9, 16]. For this reason, exact symmetries (= automorphisms) of the connectome are a simplification and an idealization. However, they should not be regarded as a falsification of symmetry



**Supplementary Figure 1. Symmetric and non-symmetric permutation.** (a) Permutation  $P$  Eq. (19) is a symmetry of the network preserving the connectivity of neurons (automorphism), and commutes with  $A$ :  $[P, A] = 0$ . (b) Permutation  $Q$  defined in Eq. (20) is not a symmetry of the network, because it changes the network connectivity by altering the weights of the links, so it does not commute with  $A$ :  $[Q, A] \neq 0$ .

principles, but rather as an intrinsic property of biological diversity. Symmetry principles, in biology, are invariably idealized and approximate: living systems do have to be sufficiently non-symmetric to evolve and diversify. Were it not so, the nature of exact symmetries would forbid any change in organisms' structure and functions. Furthermore, the animal displays a range of behaviors that are plastic and can change through learning and memory [23].

Unlike automorphisms, which are canonically defined by Eq. (18), the definition of pseudosymmetry depends on an additional parameter, a small number  $\varepsilon > 0$ , which, for our purposes, represents the 25% variation existing across animals.

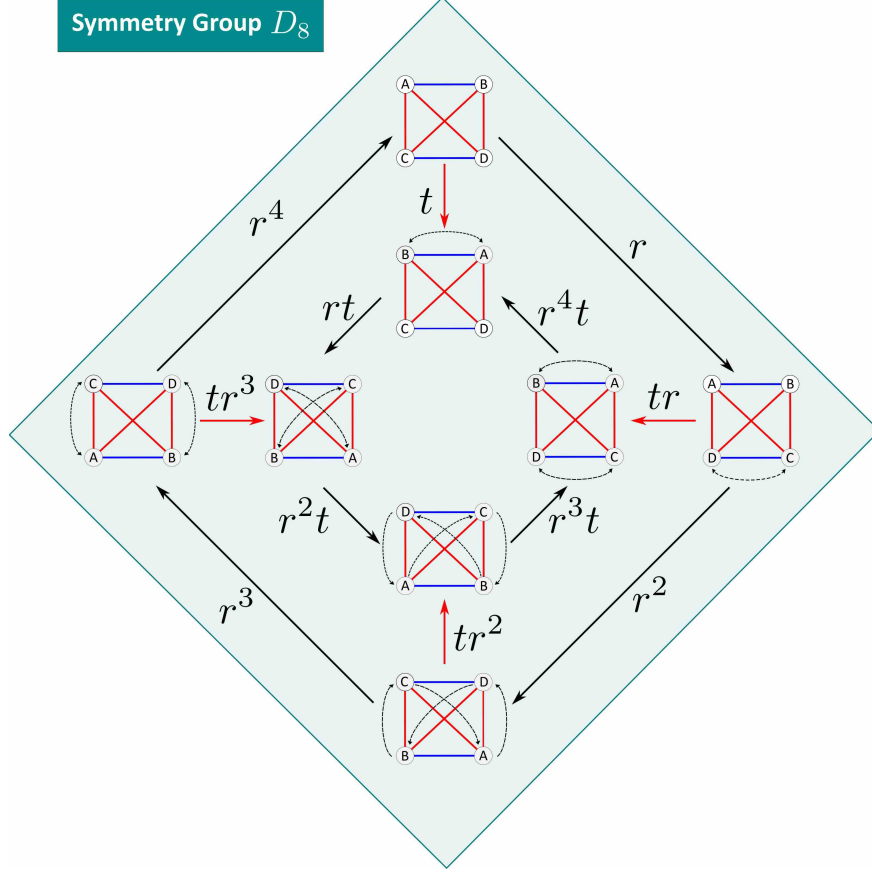
A permutation  $P_\varepsilon$  is called a pseudosymmetry if the commutator  $[P_\varepsilon, A]$  is non-zero but small

$$||[P_\varepsilon, A]|| = \varepsilon \quad (22)$$

that is,  $P_\varepsilon$  approximates an exact symmetry in the limit  $\varepsilon \rightarrow 0$ .

The norm of the commutator in Eq. (22), defined as

$$\Delta(P_\varepsilon) = ||[P_\varepsilon, A]|| \equiv \sum_{i \geq j} |A_{ij} - A_{P(i)P(j)}|, \quad (23)$$



**Supplementary Figure 2. Dihedral symmetry group  $D_8$  of the forward gap-junction circuit (interneurons only).** The automorphisms  $r$  and  $t$  are the generators of this group, as shown. The structure of this group is then converted into the system of imprimitivity when this interneuron circuit is incorporated into the whole connectome. This is a general property of all functional circuits in the connectome, to be elaborated in a follow up paper.

counts the number of links where  $P_\varepsilon$  and  $A$  do not commute. The ideal limit of classical symmetry corresponds to  $\Delta(P_\varepsilon) \rightarrow 0$ , and we recover exact automorphisms. In general, the quantity  $\Delta(P_\varepsilon) \rightarrow 0$  in Eq. (23) quantifies the deviation of  $P_\varepsilon$  from an ideal automorphism. Thus, we are lead naturally to the following definition of pseudosymmetry.

**Definition of network pseudosymmetry**– A permutation  $P_\varepsilon$  is called pseudosymmetry of the network if its deviation  $\Delta(P_\varepsilon)$  from ideal automorphism is smaller than a given indetermination constant  $\varepsilon$ , i.e.,  $\Delta(P_\varepsilon) < \varepsilon M$ , where  $M$  is the total number of links including the weights. In other words, we require pseudosymmetries to preserve at least a fraction  $(1 - \varepsilon)$  of the total number of links.



### Algorithm to find pseudosymmetries

In the present work, we choose the indetermination constant to be smaller than  $\varepsilon < 0.25$ , which represents the 25% variation in the connectivity of connectomes across animals [5, 9, 16, 17], as a condition for the permutation to be considered a pseudosymmetry. We then obtain the set of pseudosymmetries shown in the real circuits in the main text. Finding pseudosymmetries is relatively simple when the size of the network is small, because they can be determined by an exhaustive search as those permutations satisfying  $\Delta(P_\varepsilon) < M\varepsilon$ . To find the pseudosymmetries we compute for each permutation  $P$  the norm  $\Delta(P_\varepsilon)$  given by Eq. (23), and we select only those such that  $\Delta(P_\varepsilon) < M\varepsilon$ . All pseudosymmetries found in the locomotion circuits represents transformation with indetermination constant  $\varepsilon$  below 25%. The list of the indetermination constants of all subgroups appears in Table I. We notice that pseudosymmetries of locomotion circuits are, in general, highly degenerate, and their number increases as a function of  $\varepsilon$ . Due to the fact that  $\varepsilon$  is relatively small, these real circuits can then be easily symmetrized to obtain the circuits with ideal symmetries with  $\varepsilon = 0$ . This is so, since the pseudosymmetries are relatively close to a perfectly symmetric circuit. The provided ideal circuits are examples of idealized symmetrical circuit and represents the closest ideal structure to the real one and at the same time respect the same symmetries as the pseudosymmetries of the real circuit. The real circuits (and only them) and their pseudo-symmetries remain the actual circuits to be studied. When the size  $N$  of the network is larger than  $N > 20$ , finding pseudosymmetries by using an exhaustive search becomes computationally impossible. In this case, pseudosymmetries should be determined as the solutions of a constrained quadratic assignment problem, to be elaborated and described in detail in a follow up paper.

### Supplementary Note 4 - Factorization of the symmetry group

Factorization of the symmetry group into simple and normal subgroups is the fundamental tool for understanding the main results of this work. Descending to subgroups gives us useful information about the fine structure of the connectome, and eventually will allow us to identify its basic building blocks. Next, we explain the notion of subgroups and then the procedure to find the building blocks of the connectome through the factorization of its symmetry group. All definitions are standard in the group theory literature and appear in

Ref. [12].

**Definition of Subgroup**— A subset  $\mathbf{H}$  of permutations selected from a group  $\mathbf{G}$  is said to be a subgroup of  $\mathbf{G}$  if the subset  $\mathbf{H}$  forms itself a group (under the same composition law that was used in  $\mathbf{G}$ ). The concept of subgroup is fundamental in mathematics and physics since it gives the structure of fundamental forces and particles [29].

**Definition of Simple Subgroup**— A simple subgroup is a nontrivial group whose only subgroups are the trivial group and the group itself. A group that is not simple can be broken into two smaller groups, a normal subgroup and the quotient group, and the process can be repeated, as explained next.

**Definition of Normal Subgroup**— Among all subgroups of a symmetry group, the normal subgroups, Fig. 1e, are particularly significant in this work, since they allow us to define the building blocks of the connectome. A subgroup  $\mathbf{H}$  is said to be normal in a group  $\mathbf{G}$  if and only if  $\mathbf{H}$  commutes with every element  $g \in \mathbf{G}$ , i.e.,  $[g, \mathbf{H}] = g\mathbf{H} - \mathbf{H}g = 0$  (notice that the requirement is that  $\mathbf{H}$  commutes with every  $g$  as a whole subgroup, not element by element).

More precisely, consider a group  $\mathbf{G}$  and a subgroup  $\mathbf{H} \leq \mathbf{G}$ . For a given element  $g \in \mathbf{G}$  we can form the set  $\{gh : h \in \mathbf{H}\}$ , which is called the **left coset** of  $\mathbf{H}$  in  $\mathbf{G}$ . Thus we can use  $\mathbf{H}$  to generate the collection of non-overlapping cosets  $\mathbf{H}, g_1\mathbf{H}, g_2\mathbf{H}, \dots$ . Note that while  $\mathbf{H}$  is a subgroup, the cosets are, in general, simply sets. The crux of the matter is that if the cosets form themselves a group, then  $\mathbf{H}$  is called a normal subgroup. Viceversa, if  $\mathbf{H}$  is a normal subgroup, then the cosets do form a group, called the coset group. Next we explain which properties  $\mathbf{H}$  must have in order to be a normal subgroup, or equivalently, for the cosets to form a group. Let  $\mathbf{H}$  be a subgroup dividing  $\mathbf{G}$  in  $N_c$  non-overlapping cosets. Since  $\mathbf{G}$  may be, in general, a non-abelian group, the left cosets may differ from right cosets.

To be definite, in the following we consider only left cosets. Each left coset is of the form  $g\mathbf{H}$  for some  $g \in \mathbf{G}$ . Let us consider two cosets  $g_1\mathbf{H}$  and  $g_2\mathbf{H}$ . Since  $\mathbf{H}$  is a subgroup, it must contain the identity element  $e$ , i.e.  $e \in \mathbf{H}$ . Therefore  $g_1e = g_1$  is in the coset  $g_1\mathbf{H}$ . Analogously,  $g_2e = g_2$  is in the coset  $g_2\mathbf{H}$ . Now, if cosets behave like a group, then the product  $g_1g_2$  must be in the product of two cosets, that is  $g_1g_2 \in (g_1\mathbf{H})(g_2\mathbf{H})$ . Since  $g_1g_2$  is also in the coset  $g_1g_2\mathbf{H}$ , then the product of any element in the first coset with any element in the second coset should be in the coset  $g_1g_2\mathbf{H}$ , i.e.,  $(g_1\mathbf{H})(g_2\mathbf{H}) = g_1g_2\mathbf{H}$ . To see when this happens, consider an arbitrary element in the first coset  $g_1\mathbf{H}$  and call it  $g_1h_1$ , and an

element in the second coset  $g_2h_2$ . Multiplying these two elements we get  $g_1h_1g_2h_2$ . If this is in the coset  $g_1g_2\mathbf{H}$ , then this product must be equal to  $g_1g_2h_3$  for some  $h_3$ . Starting from this equation we can write:

$$\begin{aligned} g_1h_1g_2h_2 &= g_1g_2h_3 \\ h_1g_2h_2 &= g_2h_3 \\ g_2^{-1}h_1g_2h_2 &= h_3 \\ g_2^{-1}h_1g_2 &= h_3h_2^{-1} . \end{aligned} \tag{24}$$

Since  $\mathbf{H}$  is a subgroup, the right hand side of Eq. (24) is in  $\mathbf{H}$ , i.e.  $h_3h_2^{-1} \in \mathbf{H}$ . As a consequence, also  $g_2^{-1}h_1g_2$  is an element of  $\mathbf{H}$ , so we have in general that  $g_2^{-1}\mathbf{H}g_2 \in \mathbf{H}$ . In a similar way, one can prove that  $\mathbf{H} \in g_2^{-1}\mathbf{H}g_2$ , and thus conclude that

$$g_2^{-1}\mathbf{H}g_2 = \mathbf{H} \quad \rightarrow \quad [g_2, \mathbf{H}] = 0 . \tag{25}$$

To recap, we just proved that if  $\mathbf{H} \leq \mathbf{G}$  is a subgroup and the cosets form a group, then it must hold true that  $[g, \mathbf{H}] = 0$  for any  $g \in \mathbf{G}$ . In a similar way it can be proven that the converse is also true, that is, if  $[g, \mathbf{H}] = 0$  then the cosets form a group. If this happens, then  $\mathbf{H}$  is called a **normal** subgroup, denoted as  $\mathbf{H} \trianglelefteq \mathbf{G}$ , and the coset group is called **quotient** subgroup, denoted as  $\mathbf{G}/\mathbf{H}$ . Every group  $\mathbf{G}$  has at least two normal subgroups, which are the identity  $\{e\}$  and the group itself  $\mathbf{G}$ . If these are the only normal subgroups then  $\mathbf{G}$  is called a **simple group**. In other words, a simple group does not have any quotient subgroups, and for this reason simple groups represent the building blocks of other groups. Normal subgroups (and only normal subgroups) can be used to decompose the symmetry group as a direct product, as we discuss next.

**Definition of Direct Product Factorization**— To explain the factorization of a group as a direct product of normal subgroups, it is useful to introduce the following notation. Let us consider a permutation group  $\mathbf{G}$  and suppose that  $K$  is a subset of  $G$ . Then, we define the **support** of  $K$  by:

$$\text{supp}(K) = \{i \in V \mid P(i) \neq i \text{ for at least one } P \in K\} . \tag{26}$$

Then, suppose that two subsets  $\mathbf{K}$  and  $\mathbf{H}$  of a group  $\mathbf{G}$  have non-overlapping supports, that is  $\text{Supp}(K) \cap \text{Supp}(H) = \emptyset$ , then all elements in  $\mathbf{K}$  commute with those in  $\mathbf{H}$ , i.e.,  $[K, H] = 0$ . Assume now that a group  $\mathbf{G}$  can be partitioned into a collection of subsets  $\{\mathbf{H}_1, \mathbf{H}_2, \dots, \mathbf{H}_n\}$  such that for any pair  $\mathbf{H}_i$  and  $\mathbf{H}_j$ ,  $i \neq j$ ,  $\text{Supp}(\mathbf{H}_i) \cap \text{Supp}(\mathbf{H}_j) = \emptyset$ . Also, assume that each

subset  $H_i$  cannot be further partitioned into smaller subsets with non-intersecting supports. The important point is that the subsets  $\mathbf{H}_i$  found in this way are, by simple construction, the uniquely defined normal subgroups that factorize  $\mathbf{G}$  into a direct product as:

$$\mathbf{G} = \mathbf{H}_1 \times \mathbf{H}_2 \times \dots \mathbf{H}_n . \quad (27)$$

More concretely, take the sector of blue motor neurons in Fig. 4a (VB3, VB4, VB5, VB10, VB11, DB2, DB4, DB6, DB7, DB8) and its associated subgroup  $\mathbf{S}_{10}$  and the subgroup  $\mathbb{T}_F^{\text{ch}}$  which acts on the sector of touch neurons colored green PVCL and PVCR. If we apply any permutation of  $\mathbf{S}_{10}$  to the blue motor neurons, then the neurons PVCL and PVCR in the other sector are not affected. For instance, a permutation of VB3 and VB4 is a symmetry that does not affect for instance the touch sector of interneuron PVCL and PVCR. This factorization is because VB3 and VB4 are both connected to PVCL and PVCR, and this is a strong constraint on the connections. Imagine now that we loss two of the links and VB3 connects only to PVCL and VB4 only to PVCR. The resulting circuit would still be symmetric since we can still permute VB3 with VB4. But to keep the symmetry of the whole network, this permutation now triggers the permutation of PVCL and PVCR. Thus, VB3 and VB4 would belong to the touch sector together PVCL and PVCR. We see how the subgroup structure imposes hard constraints in the network connectivity. The fact that the connectivity of the network is precisely structured to create subgroups which can be factorized is an interesting result since not all groups possess this property. Furthermore the factors are aligned with different broad classification of functions. This is an indication that these subgroups have biological significance. Thus, the subgroup structure suggests the segregation of neurons in the network according to function yet allowing integration since the neurons are connected in the same circuit.

In Supplementary Note 5 we will show that both forward and backward circuits, either of gap-junctions or chemical synapses, have symmetry groups which factorize as a direct product of normal subgroups that correspond to specific broad functional categories from the Wormatlas.

## Supplementary Note 5 - Symmetry group of *C. elegans* locomotion circuit

### Forward gap-junction circuit

The real circuit with the weights of the synapses is shown in Supplementary Fig. 3. The corresponding symmetry group is factorized as a direct product of 6 normal subgroups:

$$\mathbf{F}_{\text{gap}} = [\mathbf{C}_2 \times \mathbf{C}_2] \times [\mathbf{S}_5 \times \mathbf{D}_1 \times \mathbf{C}_2 \times \mathbf{C}_2] . \quad (28)$$

The pair of subgroups  $[\mathbf{C}_2 \times \mathbf{C}_2]$  acts on the set of four interneurons (AVBL, AVBR, RIBL, RIBR), but does not move any motor neuron. For this reason, we put them together to form the composite subgroup  $\mathbb{C}_{\mathbf{F}_{\text{gap}}}$ , which we call **command subgroup of the forward gap-junction circuit** and define as:

$$\mathbb{C}_{\mathbf{F}_{\text{gap}}} = \mathbf{C}_2 \times \mathbf{C}_2 . \quad (29)$$

Similarly, the product  $[\mathbf{S}_5 \times \mathbf{D}_1 \times \mathbf{C}_2 \times \mathbf{C}_2]$  in Eq. (28) acts only on the motor neurons VB and DB, but not on the interneurons. Therefore, we put them together to form the composite  $\mathbb{M}_{\mathbf{F}_{\text{gap}}}$ , and we call it the **motor subgroup of the forward gap-junction circuit**, defined as

$$\mathbb{M}_{\mathbf{F}_{\text{gap}}} = [\mathbf{S}_5 \times \mathbf{D}_1 \times \mathbf{C}_2 \times \mathbf{C}_2] . \quad (30)$$

The formal decomposition of the circuit into the functional categories is:

$$\mathbf{F}_{\text{gap}} = \mathbb{C}_{\mathbf{F}_{\text{gap}}} \times \mathbb{M}_{\mathbf{F}_{\text{gap}}} . \quad (31)$$

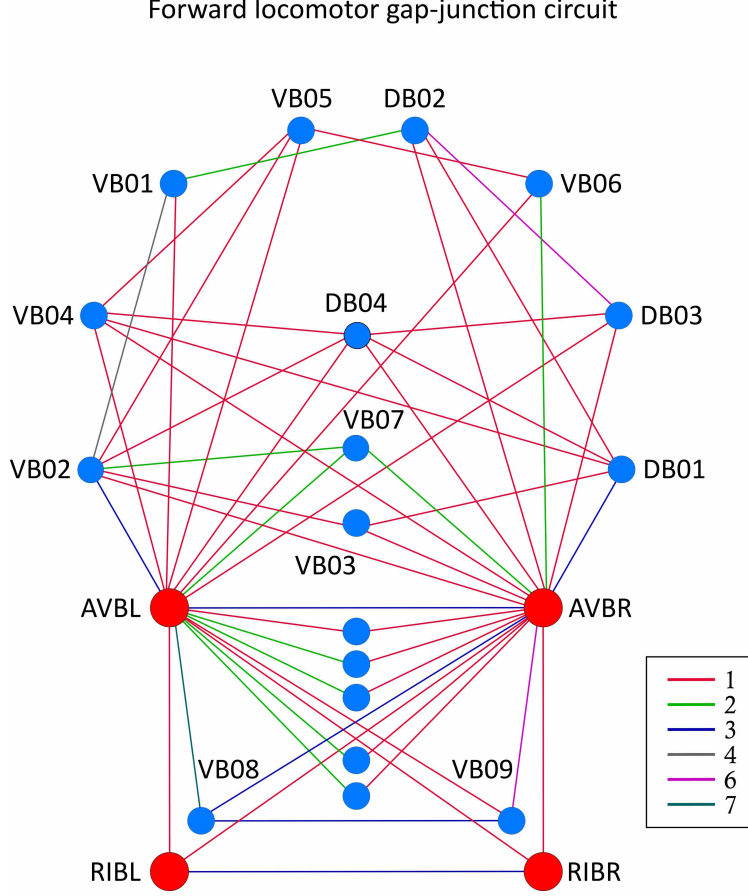
### Backward gap-junction circuit

The real circuit is shown in Supplementary Fig. 4 with the weighted links. The symmetry group of the backward circuit of gap-junctions breaks into a direct product of command and motor normal subgroups as:

$$\mathbf{B}_{\text{gap}} = (\mathbf{C}_2 \times \mathbf{C}_2 \times \mathbf{C}_2 \times \mathbf{C}_2) \times (\mathbf{S}_{12} \times \mathbf{D}_6 \times \mathbf{C}_2) . \quad (32)$$

where the command subgroup is

$$\mathbb{C}_{\mathbf{B}_{\text{gap}}} = \mathbf{C}_2 \times \mathbf{C}_2 \times \mathbf{D}_1 , \quad (33)$$



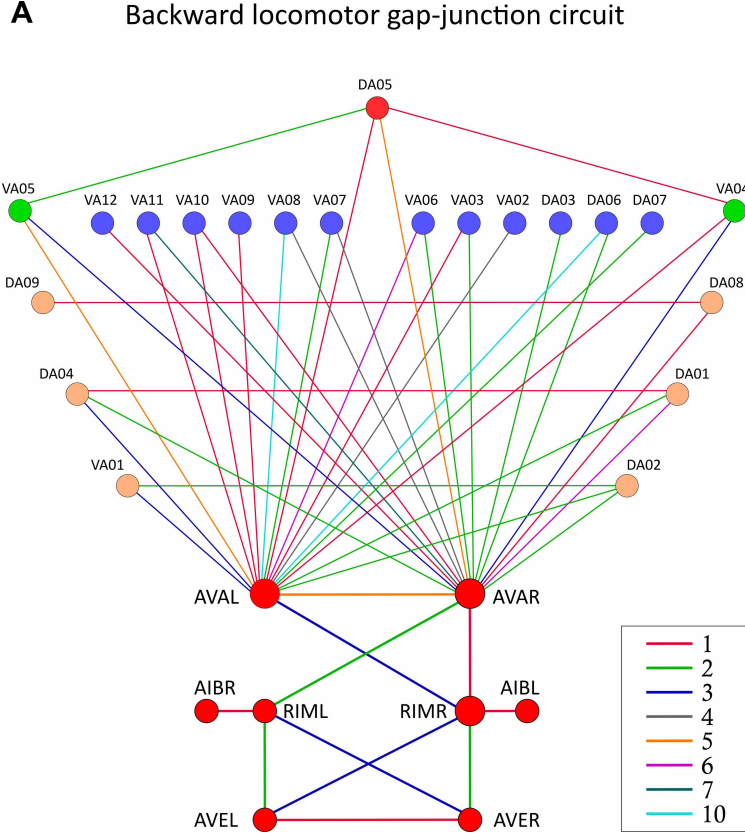
**Supplementary Figure 3. Real forward locomotion gap-junction circuit.** This circuit comprises 22 neurons divided in 2 sectors: the command-sector including the 4 interneurons (AVBL, AVBR, RIBL, RIBR); and the motor-sector including the remaining motor neurons.

acts on the command sector (AVAL, AVAR, AVEL, AVER, RIML, RIMR, AIBL, AIBR), and fix the motor sector, while the motor subgroup

$$\mathbb{M}_{\mathbf{B}_{\text{gap}}} = \mathbf{S}_{12} \times \mathbf{D}_6 \times \mathbf{C}_2, \quad (34)$$

acts only on motor neurons DA and VA and leaves the interneurons fixed. The formal decomposition of the circuit is:

$$\mathbf{B}_{\text{gap}} = \mathbb{C}_{\mathbf{B}_{\text{gap}}} \times \mathbb{M}_{\mathbf{B}_{\text{gap}}} . \quad (35)$$



**Supplementary Figure 4. Real backward gap-junction circuit.** This circuit comprises 29 neurons connected by gap-junctions. These neurons form 2 disjoint sectors: the command-sector including 8 interneurons (AVAL, AVAR, RIML, RIMR, AIBL, AIBR, AVEL, AVER); and the motor sector formed by the remaining 21 motor neurons.

### Forward chemical synapse circuit

We construct the forward circuit of chemical synapses using the same neurons of the forward gap-junction circuit discussed in Supplementary Note 5. In addition, we consider also the two neurons PVCL and PVCR, since they are connected to the other ones via chemical synapses (but not via gap-junctions). The resulting real circuit with the weighted links is displayed in Supplementary Fig. 5, and its pseudosymmetries are listed in Table I. We consider the different chemical synaptic connections according to the different neurotransmitters into excitatory and inhibitory. All neurons are cholinergic and excitatory (ACh) except for RIM which uses neurotransmitter Glutamate and Tyramine and AIB which is glutamatergic, as shown in Supplementary Table III. These different types of synaptic con-

nections do not affect the symmetries of the circuits and therefore we avoid to plot the type of neurotransmitter in the links of the chemical synapses circuits for clarity in all chemical circuits.

The corresponding (pseudo)symmetry group factorizes as the direct product of five normal subgroups in the following way:

$$\mathbf{F}_{\text{ch}} = (\mathbf{C}_2) \times (\mathbf{D}_1) \times (\mathbf{S}_{10} \times \mathbf{D}_1) , \quad (36)$$

The first subgroup  $\mathbf{C}_2$  in Eq. (36) acts only on the pair of neurons (PVCL, PVCR) and leaves the rest fixed. For this reason, we name it **touch subgroup of forward chemical synapse circuit**, and define as:

$$\mathbb{T}_{\mathbf{F}_{\text{ch}}} = \mathbf{C}_2 , \quad \text{touch subgroup.} \quad (37)$$

The subgroup  $\mathbf{D}_1$  acts only on the four interneurons, thus forming a composite subgroup named **command subgroup of the forward chemical synapse circuit**, which is defined as:

$$\mathbb{C}_{\mathbf{F}_{\text{ch}}} = \mathbf{D}_1 , \quad \text{command subgroup.} \quad (38)$$

Lastly, the pair of subgroups  $\mathbf{S}_{10} \times \mathbf{D}_1$  acts only on the motor neurons of this circuit, thus forming the **motor subgroup of the forward chemical synapse circuit**, which is defined by:

$$\mathbb{M}_{\mathbf{F}_{\text{ch}}} = [\mathbf{S}_{10} \times \mathbf{D}_1] , \quad \text{motor subgroup.} \quad (39)$$

The decomposition of this circuit is:

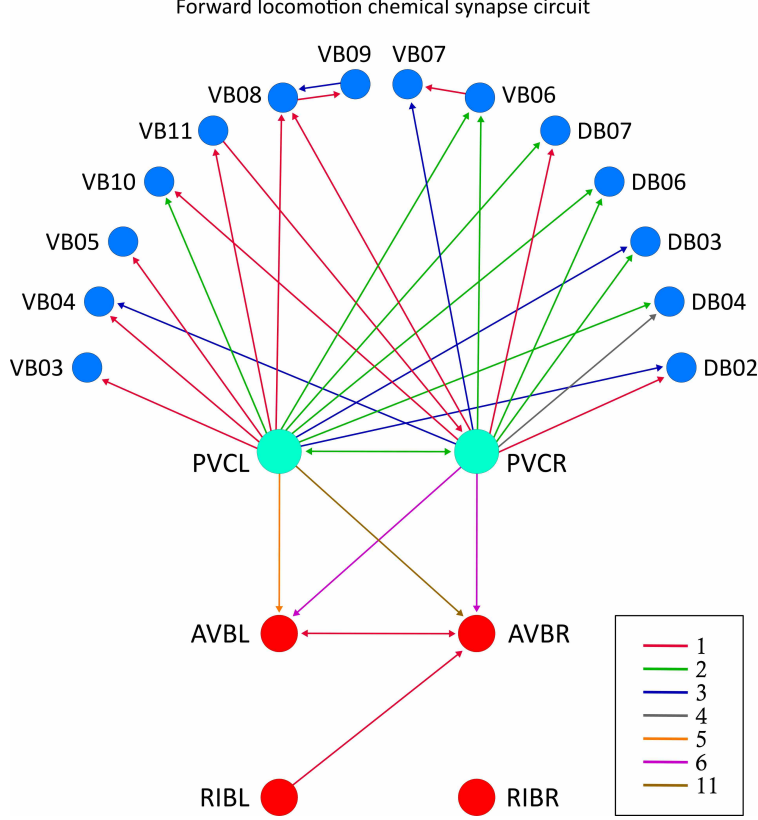
$$\mathbf{F}_{\text{ch}} = \mathbb{T}_{\mathbf{F}_{\text{ch}}} \times \mathbb{C}_{\mathbf{F}_{\text{ch}}} \times \mathbb{M}_{\mathbf{F}_{\text{ch}}} . \quad (40)$$

For simplicity we plot only the interneurons that connect to the motor neurons. Full circuit in Supplementary Fig. 6. All neurotransmitters are cholinergic and excitatory (ACh) except for RIM which uses neurotransmitter Glutamate and Tyramine and AIB which is glutamatergic (see Supplementary Note 6). These different types of synaptic interactions respect the symmetries of the circuits, see Supplementary Note 5.

### Backward chemical synapse circuit

Since this circuit has a quite dense connectivity structure, for easier visualization, we plot it by separating two parts. Supplementary Fig. 6a shows the real circuit involved in the





**Supplementary Figure 5. Real forward chemical synapse circuit.** This circuit comprises 20 neurons divided in 3 sectors: the touch-sector including the pair (PVCL, PVCR); the command-sector including the 4 interneurons (AVBL, AVBR, RIBL, RIBR); and the motor-sector including the remaining neurons. All neurons in this circuit are cholinergic.

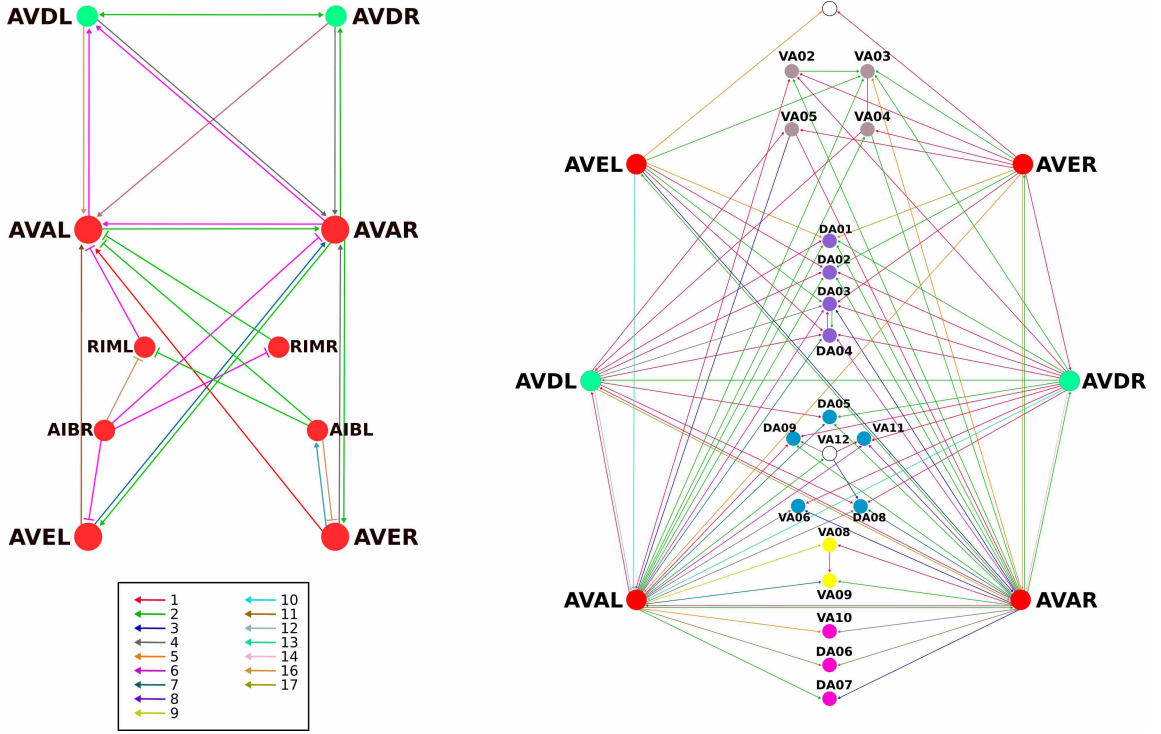
touch-command subgroups. We then add the motor neurons in the class A and replot the interneurons involved in backward locomotion but only those that connect with the motor neurons in Supplementary Fig. 6b. These are the neurons AVA, AVE and AVD. Interneurons AIB and RIM in the command subgroup are not included for clarity of visualization because they do not contribute to the connections between the different sectors. We then obtain the real circuit displayed in Supplementary Fig. 6b involved in the touch-command-motor subgroups.

The symmetry group of the backward chemical synapse circuit shown in Fig. 4c is factorized as:

$$B_{\text{ch}} = [C_2] \times [C_2 \times C_2] \times [S_5 \times S_4 \times S_3 \times C_2 \times D_1] . \quad (41)$$

The touch sensitivity subgroup is composed of neurons AVD, the command interneuron

**a** Backward chemical synapse circuit (Interneurons only) **b** Backward locomotor chemical synapse circuit (full)



**Supplementary Figure 6. Real backward chemical synapse circuit.** **a.** We plot separately the interneurons for clarity. This part of the circuit comprises 10 neurons and the chemical synapse between them. These neurons form 2 disjoint sectors: the touch-sector including the pair (AVDL, AVDR); and the command-sector including the other 8 interneurons (AVAL, AVAR, RIML, RIMR, AIBL, AIBR, AVEL, AVER). All neurons in this circuit are cholinergic and excitatory (ACh), except for RIM and AIB which are inhibitory: RIM uses neurotransmitter Glutamate and Tyramine and AIB is glutamatergic. The inhibitory nature of their synaptic connections is shown graphically by T-headed arrows ( $\neg$ , inhibitory links), as opposed to excitatory synapses represented by ordinary arrows ( $\rightarrow$ , excitatory links). The different types of synapses do not affect the pseudosymmetries of this circuit. **b.** We add the motor neurons to the circuit and plot only the interneurons that connect to the motor sector, for clarity. All neurons in this circuit are cholinergic.

subgroup of neurons AVA, AVE, AIB and RIM, and the motor subgroup consists of motor neurons VA and DA. The decomposition of this circuit is, respectively:

$$\mathbf{B}_{\text{ch}} = \mathbf{T}_{\mathbf{B}_{\text{ch}}} \times \mathbf{C}_{\mathbf{B}_{\text{ch}}} \times \mathbf{M}_{\mathbf{B}_{\text{ch}}} . \quad (42)$$

## Supplementary Note 6 - Wormatlas functional categories on neurons

Broad functional categories of neurons are provided at the Wormatlas: <http://www.wormatlas.org/hermaphrodite/nervous/Neuroframeset.html>, Chapter 2.2 [25]. A classification for every neuron into four broad neuron categories is provided as follows: (1) *'motor neurons, which make synaptic contacts onto muscle cells'*, (2) *'sensory neurons'*, (3) *'interneurons, which receive incoming synapses from and send outgoing synapses onto other neurons'*, and (4) *polymodal neurons, which perform more than one of these functional modalities'*.

The Wormatlas classifies most neurons (some of them unknown) in further functional categories as well as provides the neurotransmitters. We reproduce the information from the Wormatlas used in the main text in Supplementary Table II and Supplementary Table III.

| Forward circuit |                                |  |                  |
|-----------------|--------------------------------|--|------------------|
| Neuron          | Functional Category            | Explanation  | Neurotransmitter |
| AVB             | interneuron                    | driver cell for forward locomotion   | ACh              |
| RIB             | interneuron/motor<br>polymodal | second layer interneuron,<br>process of integration of information, locomotion           | ACh              |
| PVC             | interneuron                    | command interneuron for forward locomotion,<br>modulates response to harsh touch to tail | ACh              |
| VB              | motor (sensory)                | locomotion (ventral), proprioception   | ACh              |
| DB              | motor                          | forward locomotion (dorsal), proprioception  | ACh              |

**Supplementary Table II.** Functional categories of the neurons in the forward circuit according to the Wormatlas.

## Supplementary Note 7 - Blocks of imprimitivity

The correspondence of network building blocks and simple subgroups provides a rigorous theoretical characterization of the network connectivity structure and a natural interpretation of its broad functional categories according to the Wormatlas. However, a more accurate description of functionality should take into account also the splitting of these building blocks into finer topological structures. The fine structure corrections to the building blocks can be

| Backward circuit |                        |  |                  |
|------------------|------------------------|--|------------------|
| Neuron           | Function category      | Explanation  | Neurotransmitter |
| AVA              | interneuron            | command interneuron, locomotion,<br>driver cell for backward locomotion  | ACh              |
| AVE              | interneuron            | command interneuron,<br>drive backward movement  | ACh              |
| RIM              | interneuron<br>(motor) | second layer interneuron,<br>process of integration of information, locomotion                                 | Glu, Tyr         |
| AIB              | interneuron            | first layer amphid interneuron,<br>locomotion, food and odor-evoked behavior,<br>lifespan, starvation response | Glu              |
| AVD              | interneuron            | command interneuron,<br>modulator for backward locomotion induced by head-touch                                | ACh              |
| VA               | motor                  | locomotion   | ACh              |
| DA               | motor                  | backward locomotion  | ACh              |

**Supplementary Table III.** Functional categories of the neurons in the backward circuit according to the Wormatlas.

obtained systematically through the concept of **system of imprimitivity** of a symmetry group  $\mathbf{G}$ . All definitions appear in [12].

To define a system of imprimitivity we need first the notions of **transitivity** and **blocks**. A group  $\mathbf{G}$  is said to be **transitive** on the set of nodes  $V$  if for every pair of nodes  $i, j \in V$  there exist  $P \in \mathbf{G}$  such that  $P(i) = j$  (in other words,  $\mathbf{G}$  has only one orbit). A group which is not transitive is called intransitive. A block is defined as a non-empty subset  $\mathcal{B}$  of nodes such that for all permutations  $P \in \mathbf{G}$  we have that:

- either  $P$  fixes  $\mathcal{B}$ :  $P(\mathcal{B}) = \mathcal{B}$ ;
- or  $P$  moves  $\mathcal{B}$  completely:  $P(\mathcal{B}) \cap \mathcal{B} = \emptyset$ .

If  $\mathcal{B} = \{i\}$  or  $\mathcal{B} = \{V\}$ , then  $\mathcal{B}$  is called a trivial block. Any other block is nontrivial. If  $\mathbf{G}$  has a nontrivial block then it is called **imprimitive**, otherwise is called **primitive**.

The importance of blocks rests on the following fact. If  $\mathcal{B}$  is a block for  $\mathbf{G}$ , then  $P(\mathcal{B})$  is also a block for every  $P \in \mathbf{G}$ , and is called a conjugate block of  $\mathcal{B}$ . Suppose that  $\mathbf{G}$  is transitive on the set of nodes  $V$  and define  $\Sigma = \{P(\mathcal{B}) \mid P \in \mathbf{G}\}$  as set of all blocks conjugate to  $\mathcal{B}$ . Then the sets in  $\Sigma$  form a partition of the set of nodes  $V$ , and each element of  $\Sigma$  is a block for  $\mathbf{G}$ . We call  $\Sigma$  a **system of imprimitivity** for the (symmetry) group  $\mathbf{G}$  [12].

In the text we have shown that the action of  $\mathbf{G}$  on the system of imprimitivity  $\Sigma$  gives important information about the functionality of the neural circuits, provided  $\mathcal{B}$  is not a trivial block.

## Supplementary Note 8 - Circulant Matrices and Fast Fourier Transform

In this section we discuss the relationship between circulant matrices and discrete Fourier analysis (see Fig. 1g). In particular, we show that the eigenvalues of circulant matrices can be computed extremely fast through a routine of just  $O(N \log N)$  operations, called Fast Fourier Transform (FFT).

We start the discussion by recalling that a circulant matrix  $A = \text{circ}(a_0, a_1, \dots, a_{N-1})$  can always be written as a polynomial of the permutation matrix  $P = \text{circ}(0, 1, 0, \dots, 0)$  of degree at most  $N - 1$ , that is:

$$A = a_0 I + a_1 P + a_2 P^2 + \dots + a_{N-1} P^{N-1} . \quad (43)$$

For instance, the low-pass filter:

$$\mathcal{L} = \text{circ}(1, 1) = \begin{bmatrix} 1 & 1 \\ 1 & 1 \end{bmatrix} , \quad (44)$$

can be written as  $\mathcal{L} = I + P$ . Next, we introduce the matrix  $F$  with entries  $F_{ab}$  defined as follows:

$$F_{ab} = \frac{1}{\sqrt{N}} e^{\frac{2\pi i}{N} ab} . \quad (45)$$

Matrix  $F$  is a unitary matrix ( $F^\dagger = F^{-1}$ ) which represents the kernel of the discrete Fourier transform (DFT). Specifically, given a vector  $x$ , its DFT, denoted as  $\tilde{x}$ , is the vector defined as:  $\tilde{x}_a = \sum_b F_{ab} x_b$ . The crucial point is that the permutation matrix  $P = \text{circ}(0, 1, 0, \dots, 0)$  is diagonalized by  $F$ , that is  $P = F \Lambda F^{-1}$ . This can be easily seen by calculating explicitly

the product  $F^{-1}PF$ , which reads:

$$(F^{-1}PF)_{ab} = \frac{1}{N} \sum_{k=0}^{N-1} \sum_{m=0}^{N-1} e^{-\frac{2\pi i}{N}ak} P_{km} e^{\frac{2\pi i}{N}mb} = \frac{e^{\frac{2\pi i}{N}b}}{N} \sum_{k=0}^{N-1} e^{\frac{2\pi i}{N}k(b-a)} = \delta_{ab} e^{\frac{2\pi i}{N}b} . \quad (46)$$

As a consequence of Eq. (46), any circulant matrix  $A$  is also diagonalized by  $F$  as

$$(F^{-1}AF)_{ab} = \sum_{n=0}^{N-1} a_n (F^{-1}P^n F)_{ab} = \delta_{ab} \sum_{n=0}^{N-1} a_n e^{\frac{2\pi i}{N}nb} , \quad (47)$$

so we can write down the eigenvalues  $\{\lambda_a\}$  of  $A$  as

$$\lambda_a = \sum_{n=0}^{N-1} a_n e^{\frac{2\pi i}{N}na} , \quad a = 0, \dots, N-1 . \quad (48)$$

Eigenvalues  $\{\lambda_a\}$  can be computed efficiently using the FFT of the vector  $\vec{\alpha} \equiv \frac{1}{\sqrt{N}}(a_0, a_{N-1}, \dots, a_1)^T$ .

To see this, we rewrite  $\lambda_a$  as

$$\begin{aligned} \lambda_a &= \sum_b (F^{-1}AF)_{ab} = \sum_{bk} (F^{-1}A)_{ak} F_{kb} = \sqrt{N} \sum_k (F^{-1}A)_{ak} \delta_{k0} \\ &= \sqrt{N} (F^{-1}A)_{a0} = \frac{1}{\sqrt{N}} \sum_b F_{ab} A_{b0} , \end{aligned} \quad (49)$$

where we used the fact that  $F$  satisfies the following sum rules:

$$\begin{aligned} \sum_{b=0}^{N-1} F_{ab} &= \sqrt{N} \delta_{a0} , \\ \sum_{b=0}^{N-1} F_{ab}^{-1} F_{b0} &= \frac{1}{N} \delta_{a0} . \end{aligned} \quad (50)$$

Using the vectors  $\vec{\alpha} \equiv \frac{1}{\sqrt{N}}(a_0, a_{N-1}, a_{N-2}, \dots, a_1)^T$  and  $\vec{\lambda} \equiv (\lambda_0, \lambda_1, \dots, \lambda_{N-1})^T$ , we can write Eq (49) in the simple form

$$F\vec{\alpha} = \vec{\lambda} , \quad (51)$$

which shows that the eigenvalues  $\{\lambda_a\}$  of  $A$  are the components of the DTF of vector  $\vec{\alpha}$ . Since  $F\vec{\alpha}$  can be evaluated in  $O(N \log N)$  operations using a FFT, then the computational effort for diagonalizing a circulant matrix  $A$  requires  $O(N \log N)$  operations, too. Thus, we can interpret the functionality of the circulant matrix as a fast way (almost linear in the number of nodes) to perform a Fourier Transform for processing of information.